

Historic magmatism on the Reykjanes Peninsula, Iceland: a snap-shot of melt generation at a ridge segment

David W. Peate · Joel A. Baker · Sveinn P. Jakobsson · Tod E. Waight · Adam J. R. Kent · Nathalie V. Grassineau · Anna Cecile Skovgaard

Received: 13 February 2008 / Accepted: 26 August 2008 / Published online: 16 September 2008
© Springer-Verlag 2008

Abstract We present new compositional data on a suite of historic lava flows from the Reykjanes Peninsula, Iceland. They were erupted over a short time period between c. 940 and c. 1340 AD and provide a snap-shot view of melt generation and evolution processes beneath this onshore, 65 km long, ridge segment. The lavas are tholeiitic basalts (MgO 6.5–9.2 wt%) and sparsely ($\ll 5\%$) olivine and/or plagioclase phyric (\pm trace clinopyroxene). Individual eruptive events show remarkable compositional homogeneity. Despite a limited variation in Sr–Nd isotope compositions, high-precision double-spike Pb isotope data show tight coherent arrays that, together with correlations with incompatible trace element ratios, indicate control by binary mixing processes. Poor correlations with elemental abundances require that this mixing took place prior to

extensive fractional crystallisation. Olivines in the historic lavas have light $\delta^{18}\text{O}$ values (+4.2 to +4.3‰), which is likely to be a feature of the enriched mantle source to Reykjanes Peninsula lavas. High precision Pb isotope analyses of other post-glacial Reykjanes Peninsula lavas show significant variability in $^{207}\text{Pb}/^{204}\text{Pb}$ and $^{208}\text{Pb}/^{204}\text{Pb}$ at lower $^{206}\text{Pb}/^{204}\text{Pb}$ values than in the historic lavas. This variation demonstrates that at least three compositionally distinct components within the mantle are required to explain the Pb isotope variations within the Reykjanes Peninsula as a whole.

Keywords Iceland · Mixing · Tholeiitic basalts · High-precision Pb isotopes

Communicated by J. Blundy.

Electronic supplementary material The online version of this article (doi:10.1007/s00410-008-0339-4) contains supplementary material, which is available to authorized users.

D. W. Peate (✉)
Department of Geoscience, University of Iowa,
121 Trowbridge Hall, Iowa City, IA 52242, USA
e-mail: david-peate@uiowa.edu

J. A. Baker
School of Geography, Environmental and Earth Sciences,
Victoria University of Wellington, P.O. Box 600, Wellington,
New Zealand

S. P. Jakobsson
Icelandic Institute of Natural History, Hlemmur 3,
105 Reykjavik, Iceland

T. E. Waight
Geological Institute, University of Copenhagen,
Øster Voldgade 10, 1350 Copenhagen K, Denmark

Introduction

Mixing between compositionally distinct components is increasingly recognised as an important process in gene-

A. J. R. Kent
Department of Geosciences, Oregon State University,
104 Wilkinson Hall, Corvallis, OR 97330, USA

N. V. Grassineau
Department of Geology, Royal Holloway University of London,
Egham, Surrey TW20 0EX, UK

A. C. Skovgaard
Danish Environmental Protection Agency, 1401 Copenhagen,
Denmark

rating the compositional diversity of oceanic magmatism at various length scales, from microscopic melt inclusions in olivine crystals to suites of lavas from 100 km rift segments (e.g. Langmuir et al. 1978; Saal et al. 1998; Lundstrom et al. 1998; Kamber and Collerson 2000; Reiners 2002). In particular, high precision Pb isotope data on individual mid-ocean ridge segments and on individual volcanic systems on oceanic islands such as Iceland often preserve coherent linear trends that have been attributed to local mixing between two compositionally distinct end-members (e.g. Sims et al. 2002; Stracke et al. 2003; Thirlwall et al. 2004; Baker et al. 2004; Blichert-Toft et al. 2005).

Radiogenic isotope data demonstrate significant compositional heterogeneity in the mantle beneath Iceland and the adjacent ridges (e.g. Hart et al. 1973; Sun and Jahn 1975; Zindler et al. 1979; Condomines et al. 1983; Kurz et al. 1985; Sigmarsson et al. 1992; Hémond et al. 1993; Hanan and Schilling 1997; Hardarson et al. 1997; Hilton et al. 1999; Schilling et al. 1999; Stecher et al. 1999; Skovgaard et al. 2001; Stracke et al. 2003; Thirlwall et al. 2004, 2006; Kokfelt et al. 2006; Brandon et al. 2007). Initial models explained the isotopic variations in terms of mixing between Iceland plume mantle (high $^{87}\text{Sr}/^{86}\text{Sr}$, $^{206}\text{Pb}/^{204}\text{Pb}$, $^3\text{He}/^4\text{He}$, $\text{La}/\text{Sm}_\text{N}$ and low $^{143}\text{Nd}/^{144}\text{Nd}$) and the surrounding MORB source mantle (e.g. Hart et al. 1973). However, subsequent work has revealed more complexity in the nature and number of mixing end-member compositions that contribute to Icelandic magmatism and the surrounding ridges (Reykjanes Ridge, Kolbeinsey Ridge), with up to six distinct components suggested (e.g. Hanan and Schilling 1997; Murton et al. 2002; Thirlwall et al. 2004; Kokfelt et al. 2006). There has also been considerable debate as to whether the depleted unradiogenic component is in fact ambient North Atlantic MORB source or an intrinsic depleted component within the upwelling plume mantle (e.g. Kerr et al. 1995; Hanan and Schilling 1997; Fitton et al. 1997; Hanan et al. 2000; Kempton et al. 2000; Chauvel and Hémond 2000; Fitton et al. 2003; Stracke et al. 2003; Thirlwall et al. 2004; Kokfelt et al. 2006). High precision Pb isotope data (Thirlwall et al. 2004; Baker et al. 2004) show that in geographically restricted localities within Iceland, the isotopic variations are consistent with the involvement of two components only. How these local end-members relate to the regional-scale end-members recognised for Iceland as a whole can potentially provide information about the distribution and length scale of heterogeneities within the mantle.

In this paper, we focus on a series of very fresh, virtually aphyric basaltic lava flows that erupted in historic times (after settlement in 874 AD) along the Reykjanes Peninsula in south-west Iceland (Fig. 1). We use high-precision Pb isotope data coupled with other compositional data to

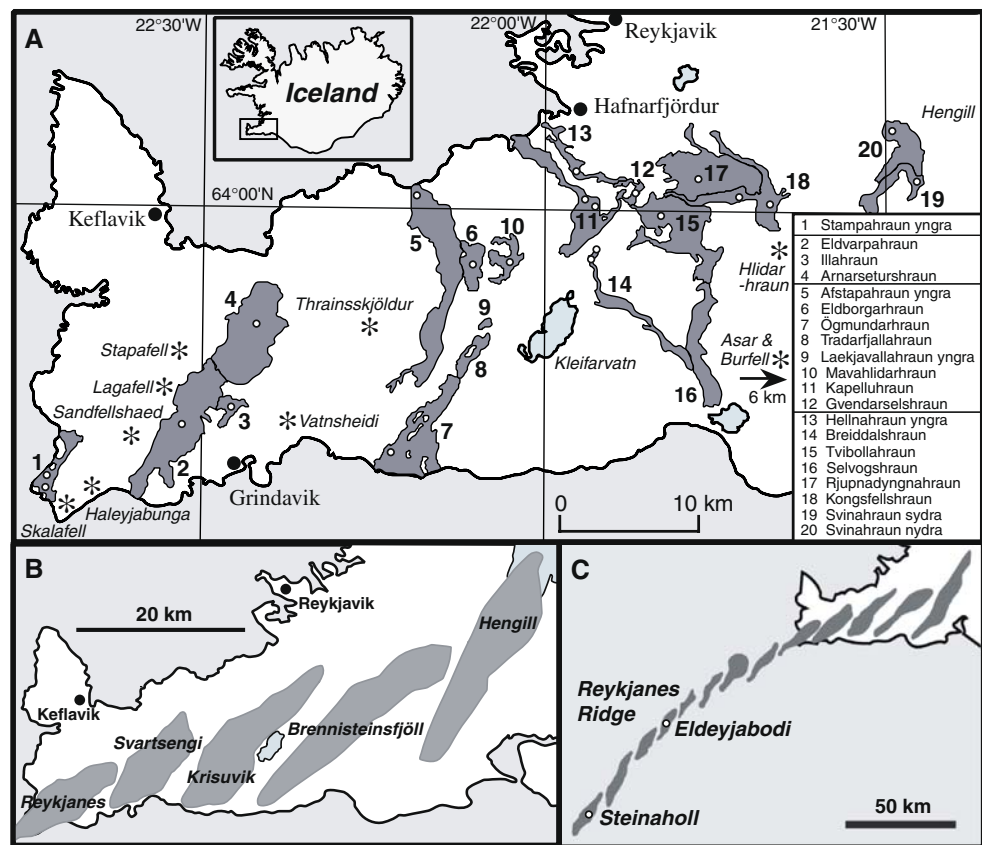
investigate the nature of mixing processes within this geographically and temporally restricted sample suite. We also evaluate the relationship of these historic lavas both to the earlier phases of magmatism on the Reykjanes Peninsula and to the adjacent offshore Reykjanes Ridge.

Geological background and sample details

The Reykjanes Peninsula in south-west Iceland represents the onshore continuation of the Reykjanes Ridge. The exposed basement volcanic rocks are all younger than 700 ka, and a significant proportion of the peninsula is covered by post-glacial (<13 ka) mafic lavas, as lava shields or fissure-fed lavas. Post-glacial magmatism occurs in a series of five en-echelon NE–SW-trending volcanic systems (fissure swarms), whose arrangement is a consequence of the obliquity of the peninsula relative to the plate spreading direction (Jakobsson et al. 1978; Gudmundsson 1986; Gee et al. 2000; Clifton and Kattenhorn 2006). From west to east, these are the Reykjanes volcanic system (partly submerged), the Svartsengi volcanic system, the Krisuvik volcanic system, and the Brennisteinsfjöll volcanic system, with the Hengill volcanic system forming the eastern edge of the Reykjanes Peninsula magmatism (Fig. 1b). The segment of rift represented by the Reykjanes Peninsula is about 65 km in length. The Hengill volcanic system continues to the north-east to the Langjökull region, forming the ~130 km long Western Volcanic Zone. The period of deglaciation (9–13 ka) was associated with greater magma production rates and the eruption of minor volumes of trace-element-depleted picritic lavas (Jakobsson et al. 1978; Gee et al. 1998a; MacLennan et al. 2002). Although many studies have focused on these unique picritic rocks (e.g. Elliott et al. 1991; Gurenko and Chaussidon 1995; Révillon et al. 1999; Chauvel and Hémond 2000; Skovgaard et al. 2001; Brandon et al. 2007), it is important to emphasize that they are not representative of the main volume of post-glacial magmatism erupted on the Reykjanes Peninsula (e.g. Jakobsson et al. 1978).

The historic lavas were erupted as fissure-fed flows within a 400 year interval from c. 940 to c. 1340 AD, based on published age constraints from historical records, tephrochronology, and ^{14}C dating (Table 1, Jónsson 1983; Einarsson et al. 1991; and references therein). Since this time, there have been no further eruptions on the peninsula itself, and magmatic activity in the region is now concentrated in the ridge segments just offshore where there have been several eruptions within the last century (e.g. Jakobsson 1974; Johnson and Jakobsson 1985). One or two samples were taken from most of the main named historical flows (Fig. 1a), although it should be noted that some of the lava flows were probably part of the same eruptive

Fig. 1 **a** Map of the Reykjanes Peninsula, Iceland, showing the historic (c. 940 to c. 1340 AD) lava flows and other localities that were sampled for this study or discussed in the text. Compiled from Jónsson (1978, 1983) and Einarsson et al. (1991). Sample locations are shown by the *white circle* symbols. *Inset* map shows location of the Reykjanes Peninsula within Iceland. **b** Magmatism in the Reykjanes Peninsula has been divided into a series of volcanic systems (fissure swarms: e.g. Jakobsson et al. 1978), and the historic lava flows are assigned to the following volcanic systems based on the locations of their eruptive vents: Reykjanes (flow 1), Svartsengi (or Grindavík: flows 2–4), Krisuvík (or Trölladyngja: flows 5–12), and Brennisteinsfjöll (or Blafjöll: flows 13–20). **c** Location of the two offshore samples from the northern Reykjanes Ridge (after Johnson and Jakobsson 1985)



events. Most samples were taken from the more massive flow interiors inside fissures, avoiding any segregation veins or pipe vesicles, although some samples are from the more vesicular flow tops. For comparative purposes, we included some additional samples in this study: (a) two samples of the recent activity offshore (Johnson and Jakobsson 1985) from a submarine hill southwest of Eldeyjarbodi ($\sim 63.5^\circ\text{N}$) and Steinaholl ($\sim 63.1^\circ\text{N}$) on the northern Reykjanes Ridge (Fig. 1c), and (b) samples of older lava flows that represent the compositional end-members on the Reykjanes Peninsula proposed by Gee et al. (1998b) (Lagafell, ~ 10 ka—‘depleted’; Stapafell, ~ 20 – 100 ka—‘enriched’, see “Discussion”). We also provide high-precision Pb isotope data on additional Reykjanes Peninsula samples from Kurz et al. (1985), Skovgaard et al. (2001) and Brandon et al. (2007) that allow us to put the historic lavas in the broader context of all Reykjanes Peninsula magmatism.

Results

Petrography and mineral chemistry

The historic lavas are sparsely phyrlic, with $\ll 5\%$ phenocrysts of olivine and/or plagioclase, and occasionally trace

amounts of clinopyroxene. Phenocryst compositions were analysed in selected samples on grain mounts of hand-picked crystals by electron microprobe in the Geological Institute, Copenhagen University, following the techniques in Larsen and Pedersen (2000). The complete data set of mineral compositions are provided in the Electronic supplementary Appendix Table A1.

Olivine

The range of olivine compositions is summarised in Fig. 2a, which plots the olivine forsterite content against the Mg# of the host sample ($\text{Mg\#} = 100 \times \text{Mg}^{2+} / (\text{Mg}^{2+} + \text{Fe}^{2+})$ assuming that $\text{Fe}^{3+} / \Sigma\text{Fe} = 0.14$, based on Mössbauer analyses of Reykjanes Peninsula glasses from Oskarsson et al. (1994). The historic lavas have olivine compositions of Fo₇₈ to Fo₈₆. Sample 456749 from Stapafell contains some olivines that have higher forsterite contents (Fo₈₂ to Fo₈₈), and the offshore sample from Eldeyjarbodi (NI-3605) has olivines with lower forsterite contents (Fo₇₅ to Fo₇₉). For most samples, the olivines have a limited range in forsterite content and they have compositions broadly expected for crystals in equilibrium with the host melt, using a $K_{\text{D}(\text{Fe}-\text{Mg})}$ value of 0.32 ± 0.04 for the distribution of Fe^{2+} and Mg between olivine and melt (Putirka 2005). However, a few samples (in particular

Table 1 Major element data (wt%) and published age estimates for Reykjanes Peninsula lavas

Sample	Lava flow (hraun)	Age	SiO ₂	TiO ₂	Al ₂ O ₃	Fe ₂ O ₃	MnO	MgO	CaO	Na ₂ O	K ₂ O	P ₂ O ₅	Vol.	Total
Historic offshore lavas (northern Reykjanes Ridge)														
NI-3605	Eldeyjarbodi 63°25'N, 23°52'W	1970–1971 AD?	49.42	1.71	13.78	14.58	0.22	6.73	10.96	2.26	0.19	0.17	0.56	99.80
NI-13958 ^a	Steinahöll 63°05'N, 24°32'W	1990 AD?	49.98	1.44	13.45	14.62	0.22	6.55	11.26	2.22	0.13	0.12	n/a	100.78
Historic 'less enriched' Reykjanes Peninsula lavas														
Reykjanes volcanic system														
456714	Stamparhraun yngra	1211–1240 AD	49.17	1.56	14.15	13.31	0.21	7.33	11.90	2.06	0.17	0.15	0.63	99.81
456716	Stamparhraun yngra	1211–1240 AD	49.05	1.38	14.74	12.64	0.20	7.53	12.11	2.05	0.15	0.14	0.78	100.24
Svartsengi volcanic system														
408673	Eldvarpahraun	1211–1240 AD	48.85	2.13	13.41	15.11	0.24	6.50	10.94	2.35	0.25	0.22	0.66	99.84
NI-8554	Illahraun	1211–1240 AD	48.59	2.01	13.66	14.58	0.23	6.91	11.25	2.35	0.23	0.20	0.59	99.71
456722	Arnarseturhraun	1211–1240 AD	48.51	1.99	13.83	14.53	0.23	6.85	11.30	2.32	0.23	0.20	0.48	100.06
Krisuvik volcanic system														
456723	Afstaparhraun yngra	1325 AD?	48.82	1.45	14.15	13.13	0.21	7.57	12.11	2.24	0.19	0.14	0.37	99.74
NI-8629	Eldborgarhraun	1325 AD?	48.75	1.49	14.04	13.28	0.21	7.67	12.10	2.14	0.18	0.13	0.54	99.69
456744	Gvendarselshraun	1151–1188 AD	48.63	1.49	14.29	13.08	0.21	7.65	12.17	2.17	0.18	0.14	0.45	99.72
456745	Kapelluhraun	1151–1188 AD	48.71	1.49	14.08	13.30	0.22	7.63	12.10	2.16	0.18	0.14	0.42	100.14
456746	Kapelluhraun	1151–1188 AD	48.63	1.51	14.25	13.04	0.21	7.66	12.18	2.21	0.18	0.14	0.45	99.75
456746 ^a	Kapelluhraun	1151–1188 AD	48.57	1.55	14.12	13.25	0.21	7.46	12.33	2.21	0.18	0.13	n/a	100.22
NI-11104	Mavahlidarhraun	1151–1188 AD	48.70	1.55	14.08	13.37	0.21	7.54	12.07	2.15	0.19	0.14	0.59	99.73
408666	Ögundarhraun	1151–1188 AD	48.75	1.48	14.23	13.05	0.21	7.66	12.14	2.15	0.19	0.14	0.60	100.13
Historic 'more enriched' Reykjanes Peninsula lavas														
Brennisteinsfjöll volcanic system														
456747	Hellnahraun yngra	940–980 AD	47.71	1.71	15.20	12.52	0.20	8.08	12.06	2.15	0.21	0.17	0.37	99.62
456733	Breiddalshraun	940–980 AD	47.67	1.66	15.22	12.63	0.20	8.01	12.05	2.19	0.20	0.17	0.40	100.02
456732	Breiddalshraun	940–980 AD	47.82	1.73	15.00	12.73	0.20	7.90	12.09	2.16	0.21	0.17	0.45	99.79
456743	Tvibollahraun	940–980 AD	47.87	1.71	15.23	12.30	0.20	8.04	12.08	2.18	0.21	0.18	0.33	99.59
456742	Rjupnadyngnahraun	1150 AD?	47.74	1.62	15.13	12.60	0.20	8.23	11.97	2.16	0.20	0.15	0.39	100.03
456740	Kongsfellshraun	1200 AD?	47.47	1.79	14.97	13.01	0.20	8.13	11.78	2.24	0.24	0.18	0.37	99.77
456741	Kongsfellshraun	1200 AD?	47.57	1.79	14.95	12.98	0.20	8.14	11.79	2.18	0.23	0.18	0.29	99.86
456737	Svinhraun sydra	1000 AD	47.15	1.84	14.72	13.28	0.20	8.83	11.42	2.13	0.23	0.19	0.33	99.59
456736	Svinhraun nydra	1000 AD	47.37	1.72	14.67	12.81	0.20	9.18	11.51	2.13	0.22	0.17	0.30	99.66
Stapafell subglacial lava (~20–100 ka)—'enriched' Reykjanes Peninsula lava														
456712 ^a	Stapafell	20–100 ka	47.27	1.86	14.74	12.42	0.19	8.29	12.77	2.00	0.27	0.20	n/a	100.10
456749 ^a	Stapafell (matrix)	20–100 ka	46.57	1.60	13.41	12.44	0.19	12.25	11.37	1.76	0.23	0.18	n/a	99.73

Table 1 continued

Sample	Lava flow (hraun)	Age	SiO ₂	TiO ₂	Al ₂ O ₃	Fe ₂ O ₃	MnO	MgO	CaO	Na ₂ O	K ₂ O	P ₂ O ₅	Vol.	Total
456749 g	Stapafell (glass: n = 7)	20–100 ka	48.22	1.78	15.11	11.65	0.16	8.30	12.37	2.14	0.27	n/a	n/a	100.00
Data quality														
XRF analyses of Krisuvik Fires (1151–1188 AD) lavas		Mean (n = 5)	48.68	1.50	14.19	13.17	0.21	7.63	12.13	2.17	0.18	0.14		
		2 SD (σ_o)	0.11	0.06	0.20	0.31	0.01	0.10	0.09	0.05	0.01	0.00		
Long term precision of XRF		2 SD (σ_r)	0.30	0.03	0.10	0.20	0.01	0.10	0.03	0.10	0.01	0.01		
Signal to noise		σ_o/σ_r	0.35	1.86	1.98	1.55	1.49	1.01	1.55	0.50	1.10	0.00		

All analyses (except those marked by superscript a) by X-ray fluorescence spectrometry on glass disks prepared with a sodium tetraborate flux (except Na₂O by atomic absorption spectrometry) at the Rock Geochemical Laboratory of the Geological Survey of Denmark and Greenland, Copenhagen. Details of analytical procedures and data quality can be found in Kystøl and Larsen (1999). All samples were powdered in an Spex alumina terna mill. 'Vol.' denotes 'volatiles' and is calculated as the loss on ignition corrected for the calculated gain of weight due to Fe oxidation during ignition (Kystøl and Larsen 1999). Analyses marked by superscript a were measured by ICP-AES at Boston University, following the methods described in Murray et al. (2000). Major element data are presented on a volatile-free basis normalised to 100% with total Fe as Fe₂O₃(t), and the totals given are the measured values. 456749g is average analysis of glass shards by electron microprobe—see Electronic Appendix Table A1c for individual analyses. n/a = not analysed. Long term precisions for the XRF analyses are based on replicate analyses of internal standards and the values are taken from Kystøl and Larsen (1999)

456746 and 456749) contain some crystals with significantly higher forsterite contents than expected for equilibrium compositions, and these represent either relicts from an earlier stage in the differentiation of the magma or xenocrysts from earlier magmatic episodes.

Plagioclase

The range of plagioclase phenocryst compositions is summarised in Fig. 2b, which plots the plagioclase anorthite content against the Mg-number of the host sample. Phenocryst compositions vary between An₇₁ and An₉₁, with most lying between An₇₅ and An₈₈, and this is similar to the range found by Jakobsson et al. (1978) for post-glacial fissure lavas on the Reykjanes Peninsula (An₆₈–An₈₈). Plagioclase phenocrysts show minor normal zoning with rim-core variations in An content of 1–4%.

Clinopyroxene

This phase was only found as a phenocryst in three samples (456714, 456746, 456722), and crystals were <1 mm in size. Clinopyroxenes were only analysed in two samples (456714, 456746). They have broadly similar compositions (En_{44–52}Fs_{9–12}Wo_{37–43} and TiO₂ ~0.5%), although those in sample 456746 have slightly higher Mg-numbers (83.5 ± 1.4, 1 SD) and lower Al₂O₃ (3.1 ± 0.6 wt%, 1 SD) than those in 456714 (81.7 ± 0.9 and 3.7 ± 0.4 wt%, respectively).

Major and trace element data

Major and trace element data are presented in Tables 1 and 2, with analytical details given in the table footnotes. The historic lavas are tholeiitic basalts, with a relatively restricted range in MgO contents (6.5–9.2 wt%) when compared with the compositional range of all recent (<20 ka) Reykjanes Peninsula lavas (Fig. 3). In most cases, lava flows that belong to the same eruptive episode show remarkable compositional homogeneity that does not greatly exceed the analytical uncertainties. This is highlighted by the average composition listed for the Krisuvik Fires eruptive episode (1151–1188 AD) in Tables 1 and 2, for which the signal to noise ratio (the variability of five separate samples divided by the precision of the analytical method based on replicate analyses) is less than two for all elements except for Rb, La and Ce. Other flows from the Krisuvik volcanic system, including the Eldborgarhraun and Afstapahraun yngra flows with slightly younger inferred ages (c. 1325 AD), have indistinguishable compositions to the Krisuvik Fires flows. For these two flows, the compositional deviations for all elements from the mean composition of the Krisuvik Fires flows are all within the 2

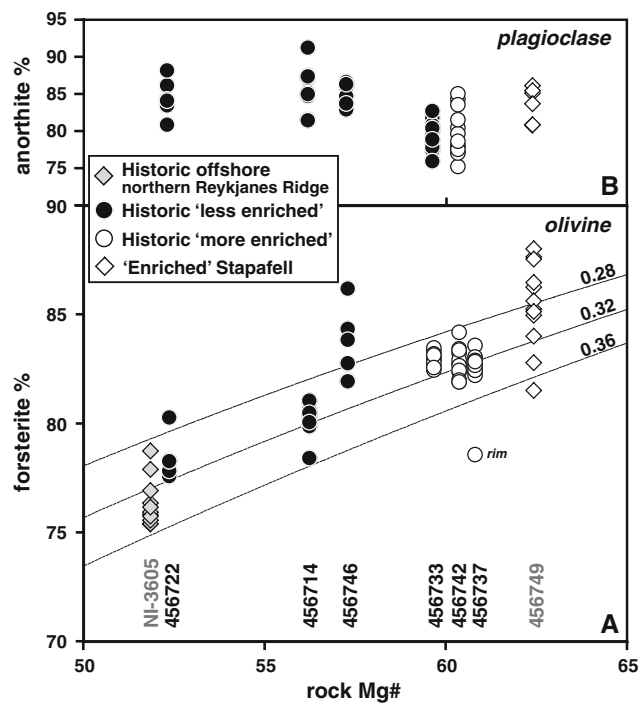


Fig. 2 **a** Olivine (Fo%) versus whole rock Mg-number (Mg#) of the host lava. Mg# [molar $100 \times \text{Mg}^{2+}/(\text{Mg}^{2+} + \text{Fe}^{2+})$] is calculated with $\text{Fe}^{3+}/\Sigma\text{Fe} = 0.14$ (Oskarsson et al. 1994). The lines indicate the compositions of olivine in equilibrium with a melt of a given Mg-number, assuming a $K_{D(\text{Fe}-\text{Mg})}$ value of 0.32 ± 0.04 for the distribution of Fe^{2+} and Mg^{2+} between olivine and melt (Putirka 2005). **b** Plagioclase (An %) versus whole rock Mg# of the host lava

SD analytical precision or the 2 SD measured variability for the Krisuvik Fires flows, except for Sr. Jakobsson et al. (1978) and Gee et al. (2000) have documented other examples of the compositional homogeneity of tholeiitic basaltic flows on the Reykjanes Peninsula. These observations are consistent with previous studies of lava flows elsewhere in Iceland (e.g. Sigmarsson et al. 1991; MacLennan et al. 2003a) that suggest that the more evolved flows (i.e. <8 wt% MgO) tend to have a more restricted compositional range, presumably due to longer residence times in the magmatic plumbing system that allows for more thorough homogenisation of magma batches. For the Reykjanes Fires episode (1211–1240 AD), the Stampahraun flow is compositionally different from the other three units that are all inferred to have been part of this eruptive episode, and it was erupted from a different volcanic system (Fig. 1).

Samples from the Reykjanes Peninsula as a whole span a wide range in incompatible trace element ratios: for example Nb/Zr varies from 0.01 to 0.18 (Fig. 4b) and La/Sm_N varies from 0.28 to 1.65 (Fig. 4a). Gee et al. (1998b) divided the samples into 'depleted' (Nb/Zr <0.08) and 'enriched' (Nb/Zr >0.08) groups. All of the historic lavas fall into the 'enriched' group, with high Nb/Zr (0.10–0.14)

and LREE-enriched compositions. For convenience, we divide the historic lavas into two arbitrary groups based on differences in trace element characteristics, namely a 'less enriched' group (Nb/Zr 0.10–0.13; La/Sm_N 1.21–1.36) and a 'more enriched' group (Nb/Zr 0.13–0.14; La/Sm_N 1.38–1.48). The 'less enriched' group show trends of increasing TiO₂ and K₂O with decreasing MgO, and the 'more enriched' group are displaced above these trends to higher MgO, TiO₂ and K₂O (Fig. 3). The 'less enriched' group also has higher SiO₂ (48.5–49.2 wt%) than the 'less enriched' group (47.2–47.9 wt%).

The 'more enriched' group are all found in the east of Reykjanes Peninsula within the Brennisteinsfjöll volcanic system, while the 'less enriched' group are found to the west in the Reykjanes, Svartsengi, and Krisuvik volcanic systems. These systematic spatial compositional variations in the historic lavas are shown in Fig. 5. For example, within the 'more enriched' group, the flows with the highest Nb/Zr are found in the extreme east of the peninsula, while in the 'less enriched' group, the flows with the lowest Nb/Zr are found in the extreme west of the peninsula in the Reykjanes volcanic system, and the historic offshore lavas in the northern Reykjanes Ridge have even lower Nb/Zr.

Radiogenic isotope data (Pb–Sr–Nd)

High precision Pb isotope data and Sr–Nd isotope data on selected samples are presented in Tables 3 and 4, with complete analytical details provided in the table captions. The historic Reykjanes Peninsula samples show a restricted range in radiogenic isotope compositions compared to the isotopic variation of all post-glacial lavas from the Reykjanes Peninsula (Fig. 6: data sources are listed in figure caption). The variations in $^{87}\text{Sr}/^{86}\text{Sr}$ (0.70309–0.70314) and ϵNd (+7.3 to +7.8) are barely outside of external analytical reproducibility (see Table 4 caption). In contrast, high-precision Pb isotope data, analysed by multi-collector inductively coupled plasma mass spectrometer (MC-ICP-MS) using a ^{207}Pb – ^{204}Pb double spike to control mass fractionation (Baker et al. 2004), show significant variations ($^{206}\text{Pb}/^{204}\text{Pb}$ 18.771–18.881; external reproducibility is $<\pm 0.003$). Furthermore, the data on the historic lavas preserve coherent linear trends on Pb–Pb isotope plots (Fig. 6b, d). The data plot below but parallel to the NHRL (Northern Hemisphere Reference Line: Hart 1984) for $^{207}\text{Pb}/^{204}\text{Pb}$ (i.e. negative $\Delta^{207}\text{Pb}$: Fig. 6a) and above but at a shallower slope to the NHRL for $^{208}\text{Pb}/^{204}\text{Pb}$ (i.e. positive $\Delta^{208}\text{Pb}$: Fig. 6c). Pb isotope data were measured on rock chips after leaching in 6 M HCl for ~2 h. Baker et al. (2004, 2005) have demonstrated the robustness of this leaching procedure to recover magmatic Pb isotope compositions from young basaltic rocks. The external precision

Table 2 Trace element data (ppm) for Reykjanes Peninsula lavas

Sample	Sc	V	Cr	Co	Ni	Cu	Zn	Ga	Rb	Sr	Y	Zr	Nb	Ba	La	Ce	Pr	Nd	Sm	Eu	Gd	Dy	Er	Yb	Lu	
Historic offshore lavas (northern Reykjanes Ridge)																										
NI-3605	52	435	151	56	75	132	124	20	2.8	117	33.5	87.6	9.1	40.2	6.18	15.70	2.29	11.48	3.50	1.27	4.60	5.40	3.46	3.26	0.49	
NI-13958 ^a	50	402	63	56	59	131	108	17	2.5	88	33.3	74.2	6.1	31.5	4.47	11.45	1.78	8.98	2.98	1.07	4.04	5.09	3.42	3.34	0.50	
NI-13958 ^b	46	379	56	51	54	128	103	17	1.6	86	31.3	73.5	6.0	29.5	4.35	11.47	1.69	8.56	2.76	0.95	4.00	4.81	3.11	3.13	0.49	
Historic 'less enriched' Reykjanes Peninsula lavas																										
Reykjanes volcanic system																										
456714	47	374	174	50	82	164	105	20	2.7	134	28.3	79.2	8.9	47.6	6.16	15.45	2.22	10.89	3.20	1.16	4.07	4.61	2.89	2.69	0.40	
456716	44	323	203	47	88	138	88	18	2.6	138	25.7	70.2	8.1	47.3	5.34	13.58	1.93	9.52	2.78	1.03	3.54	4.04	2.55	2.37	0.35	
Svartsengi volcanic system																										
408673	51	467	124	56	65	167	124	20	4.3	156	35.3	108	13.5	66.8	9.19	22.66	3.25	15.46	4.36	1.53	5.38	5.88	3.61	3.33	0.49	
NI-8554	49	432	169	53	74	165	126	22	3.7	161	33.3	105	13.1	60.5	8.61	21.21	3.02	14.42	4.04	1.44	5.01	5.44	3.27	3.03	0.46	
456722	47	423	175	52	72	166	128	23	3.7	163	32.8	103	12.9	64.6	8.69	21.42	2.97	14.53	4.09	1.45	5.01	5.46	3.34	3.05	0.45	
Krisuvik volcanic system																										
456723	53	383	111	54	84	169	103	18	2.9	147	25.8	69.2	8.9	53.7	6.11	14.95	2.15	10.27	2.96	1.10	3.76	4.22	2.64	2.45	0.36	
NI-8629	51	379	120	55	84	170	111	21	3.1	148	25.8	71.2	9.0	59.3	6.29	15.49	2.20	10.43	3.06	1.12	3.736	4.22	2.62	2.43	0.37	
456744	51	375	149	53	86	160	105	20	3.2	154	26.1	72.3	9.2	58.3	6.20	15.10	2.16	10.46	3.05	1.123	3.85	4.37	2.72	2.48	0.37	
456745	50	376	123	54	81	173	112	20	3.0	151	26.3	71.5	8.9	57.9	6.28	15.09	2.15	10.45	2.99	1.13	3.76	4.33	2.75	2.50	0.37	
456746	48	362	144	52	84	171	110	21	2.9	154	25.4	71.7	9.4	55.8	6.23	15.39	2.16	10.55	3.03	1.12	3.79	4.23	2.60	2.39	0.35	
456746 ^a	46	351	128	52	82	174	93	17	2.0	156	25.0	73.7	9.2	46.6	6.27	15.75	2.19	10.38	2.91	1.02	3.77	4.09	2.44	2.35	0.36	
NI-11104	50	381	129	54	85	158	103	18	3.1	152	26.6	75.0	9.3	55.7	6.89	16.45	2.29	11.02	3.17	1.16	3.94	4.44	2.71	2.48	0.38	
408666	50	374	143	54	89	166	98	19	3.2	155	26.0	72.9	9.1	58.9	6.33	15.55	2.23	10.64	3.06	1.14	3.82	4.26	2.63	2.42	0.36	
Historic 'more enriched' Reykjanes Peninsula lavas																										
Brennisteinsfjöll volcanic system																										
456747	42	340	309	50	112	142	99	19	3.4	195	25.1	85.3	11.8	63.6	7.58	18.32	2.56	12.22	3.42	1.24	4.04	4.27	2.52	2.29	0.33	
456733	44	347	324	53	112	139	104	20	3.3	193	24.3	83.8	11.5	62.3	7.74	18.98	2.64	12.65	3.47	1.27	4.01	4.39	2.57	2.31	0.35	
456732	43	339	309	48	104	146	99	20	3.3	194	25.3	87.3	11.7	66.6	7.62	19.02	2.62	12.51	3.43	1.26	4.09	4.24	2.50	2.23	0.33	
456743	45	351	328	52	113	143	100	19	3.6	194	24.9	85.7	12.0	62.7	7.81	18.98	2.65	12.56	3.41	1.25	4.05	4.15	2.45	2.18	0.32	
456742	45	343	324	53	120	152	100	20	3.1	192	24.6	80.7	10.8	61.3	7.13	17.46	2.49	11.73	3.24	1.19	3.88	4.12	2.45	2.20	0.33	
456740	45	359	304	53	119	151	108	22	4.0	201	25.4	90.5	12.4	65.4	8.28	20.12	2.77	13.20	3.58	1.30	4.21	4.24	2.48	2.21	0.33	
456741	43	345	296	51	114	157	96	19	3.8	204	25.8	90.2	12.1	67.1	8.21	19.54	2.76	13.06	3.52	1.29	4.23	4.40	2.62	2.32	0.35	
456737	42	353	361	55	155	147	106	19	4.0	201	26.3	95.6	13.4	65.7	8.76	21.23	2.89	13.87	3.71	1.34	4.33	4.42	2.58	2.30	0.34	
456736	42	342	429	56	168	144	111	21	3.8	191	24.8	88.7	12.3	63.0	8.14	19.75	2.74	12.98	3.50	1.26	4.16	4.23	2.50	2.19	0.32	
Stapatell subglacial lava (~20–100 ka)—'enriched' Reykjanes Peninsula lava																										
456712 ^b	42	312	403	47	118	145	89	16	4.0	200	24.6	104	16.8	74.3	10.3	24.99	3.39	15.28	3.84	1.28	4.47	4.37	2.46	2.27	0.346	
456749 ^b	37	279	670	61	309	134	91	15	3.2	186	21.5	92.3	14.7	64.2	9.01	21.78	2.98	13.43	3.38	1.13	3.94	3.84	2.16	2.00	0.312	
456749 ^g	39	287	593	59	270	140	92	16	4.8	192	23.2	94.7	14.8	72.2	9.26	21.77	3.06	13.71	3.56	1.26	3.87	3.90	2.29	2.03	0.298	
Other post-glacial (<13 ka) Reykjanes Peninsula lavas																										
408672	26	118	1914	97	983	79	51	7	0.1	35.6	7.8	9.13	0.34	2.07	0.32	1.05	0.20	1.30	0.56	0.25	0.89	1.19	0.77	0.79	0.13	

Table 2 continued

Sample	Sc	V	Cr	Co	Ni	Cu	Zn	Ga	Rb	Sr	Y	Zr	Nb	Ba	La	Ce	Pr	Nd	Sm	Eu	Gd	Dy	Er	Yb	Lu
Data quality																									
Copenhagen XRF and ICP-MS/ID analyses of Krisuvik Fires (1151-1188 AD) lavas ($n = 5$)																									
Mean	50	374	138	53	85	166	106	20	3.1	153	26.1	72.7	9.2	57.3	6.39	15.52	2.20	10.62	3.06	1.13	3.83	4.33	2.68	2.45	0.37
2 SD (σ_c)	2	14	22	2	6	13	11	2	0.3	3	0.9	2.8	0.4	3.0	0.57	1.12	0.12	0.47	0.13	0.03	0.14	0.17	0.13	0.09	0.02
Precision (%)	10	10	10	8	4	10	10	10	4	2	10	4	4	4	3	3	3	3	3	3	3	3	3	3	3
2 SD (σ_t)	5	37	14	4	3	17	11	2	0.1	3	2.6	2.9	0.4	2.3	0.19	0.47	0.07	0.32	0.09	0.03	0.11	0.13	0.08	0.07	0.01
σ_c/σ_t	0.44	0.38	1.60	0.42	1.71	0.79	1.06	1.16	2.12	1.07	0.34	0.97	1.05	1.29	2.99	2.4	1.84	1.47	1.46	0.95	1.20	1.30	1.59	1.27	2.08

Trace elements (Sc, V, Cr, Co, Ni, Cu, Zn, Ga, Rb, Sr, Y, Zr, Nb, Ba) were analysed directly on pressed powder pellets in the Department of Petrology, Geological Institute, Copenhagen University, by X-ray fluorescence using a Philips PW 1400 spectrometer and the techniques of Norrish and Chappell (1967). Results were corrected for background interference from tube and sample spectral lines, and for matrix variation (using the major element composition). USGS standards (G-2, GSP-1, AGV-1, W-1, BCR-1, PCC-1, DTS-1, W-2, DNC-1, BIR-1) were used for calibration. Rare earth elements (REE) were analysed by isotope dilution using the method of Baker et al. (2002), except for a few samples that were only analysed by ICP-MS at the Rock Geochemical Laboratory of the Geological Survey of Denmark and Greenland, Copenhagen. For these samples, the ICP-MS REE data were calibrated using the isotope dilution data on samples analysed by both methods. A few additional samples were analysed for all trace elements by ICP-MS (Open University, Boston University), and the full analyses and analytical details are given in the Electronic supplementary Table A2. Analytical precisions for the XRF trace elements are taken from Holm et al. (2006). The analytical precision for the REE elements is conservatively estimated at $<3\%$ 2σ .

Analysis of 408672 is from Skovgaard et al. (2001), with new isotope dilution REE data

of the double-spike method for Pb isotope ratios is $< \sim 150$ ppm for basaltic samples and $< \sim 400$ ppm for the low Pb concentration (sub-0.2 ppm) picritic samples (Thirlwall et al. 2004; Baker et al. 2004, 2005) based on replicate analyses of individual leached samples. There is good agreement between our double-spike data and those in Thirlwall et al. (2004) on samples from the same flows: e.g. Ögmundarhraun, Haleyjabunga, Stapafell and Lagafell (Table 3). The difference between the average composition of each flow (where more than one sample was analysed per flow) from both studies is < 500 ppm for all Pb isotope ratios.

Stable isotope data ($\delta^{18}\text{O}$)

Hand-picked olivine and/or plagioclase separates (~ 1.7 mg aliquots) from selected samples were measured for oxygen isotopes at Royal Holloway University of London using a laser fluorination technique (Mattey and Macpherson 1993; Thirlwall et al. 2006). The data are provided in Table 4, and further analytical details are given in the table footnote. The sparsely phytic nature of many of the historic lavas limited the number of samples that could be analysed. All olivines in the historic lavas have light $\delta^{18}\text{O}$ (+4.2 to +4.3‰) compared to values expected for olivines in equilibrium with normal mantle ($+5.2 \pm 0.3\%$; Mattey et al. 1994). One sample of a more primitive depleted older Reykjanes Peninsula lava (408672) from Skovgaard et al. (2001) gave a heavier $\delta^{18}\text{O}$ of +5.15‰, very different from the more extreme value of +5.62‰ determined by Skovgaard et al. (2001), but within error of the revised value for this sample of +5.08‰ measured by Thirlwall et al. (2006). An analysis of olivine from an enriched Stapafell sample gave $\delta^{18}\text{O}$ of 4.77‰, consistent with the values of +4.77 to +4.83‰ determined on a different sample from Stapafell by Thirlwall et al. (2006). Plagioclase in three of the historic lavas have $\delta^{18}\text{O}_{\text{pl}}$ of +5.03 to +5.13‰, while replicate analyses of another sample (456714) have higher $\delta^{18}\text{O}_{\text{pl}}$ of +5.40 and +5.58‰. These values are consistent with the published range for other Reykjanes Peninsula lavas of +4.51 to +5.66‰ ($+5.14 \pm 0.29\%$, 1 SD, $n = 23$; Thirlwall et al. 2006). For the three samples where both olivine and plagioclase were analysed, the isotopic fractionation for the olivine–plagioclase pairs ($\Delta^{18}\text{O}_{\text{pl-ol}}$) are +0.7‰ (456742), +0.9‰ (456733) and $\sim +1.3\%$ (456714). The value for sample 456714 is outside of the range of other Icelandic basalts ($\Delta^{18}\text{O}_{\text{pl-ol}} = 0.58 \pm 0.24$ and $0.65 \pm 0.28\%$) as determined by Thirlwall et al. (2006) and Eiler et al. (2000), respectively, which indicates disequilibrium between these two phases, most likely due to xenocrystic or antecrystic plagioclase. Plagioclase in these samples have compositions mostly between An_{75} and An_{85} ,

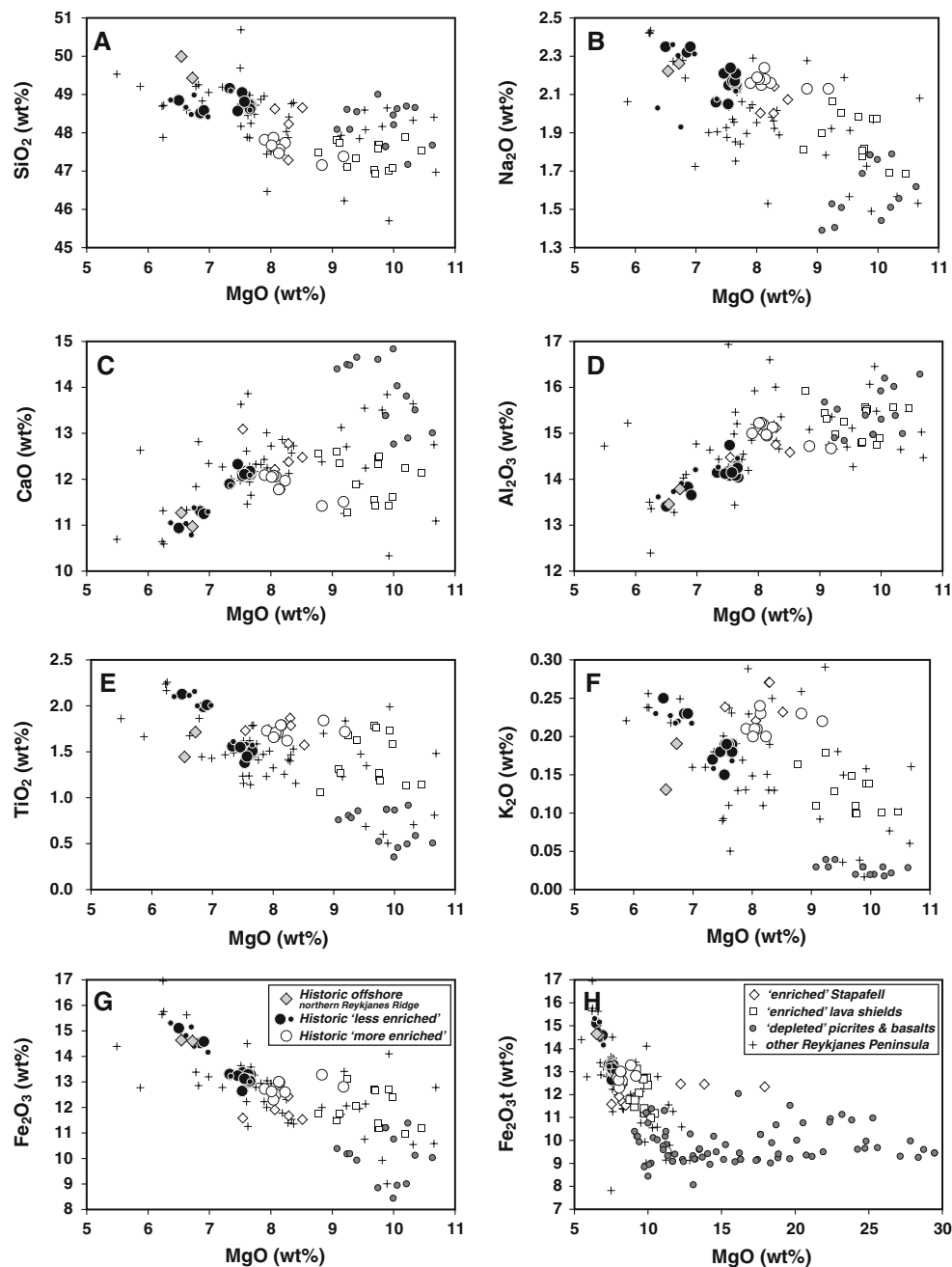


Fig. 3 Major element variation diagrams for the historic Reykjanes Peninsula lavas: MgO versus **a** SiO₂, **b** Na₂O, **c** CaO, **d** Al₂O₃, **e** TiO₂, **f** K₂O, **g–h** Fe₂O₃(t). Published literature data for other Reykjanes Peninsula lavas are shown for reference (Jakobsson et al. 1978; Wood 1978; Condomines et al. 1983; Elliott et al. 1991; Hémond et al. 1993; Gurenko and Chaussidon 1995; Gee et al. 1998b; Révillon et al. 1999; Skovgaard et al. 2001; Martin and Sigmarrsson 2005; Kokfelt et al. 2006). Small black circles are published analyses of the historic ‘less enriched’ group. **h** MgO versus Fe₂O₃(t) has an expanded scale to show the full compositional diversity of the Reykjanes Peninsula lavas, notably the trace element depleted basaltic and picritic lavas as exemplified by samples from

Haleyjabunga, Lagafell, Burfell, Asar, and Vatnsheidi (Fig. 1a). The ‘enriched’ lava shields (volumetrically dominated by the Sandfellshæd and Thrainsskjöldur shields; Fig. 1a) represent about two-thirds of the total volume of post-glacial magmas erupted on the Reykjanes Peninsula, and they were erupted shortly after the deglaciation interval that produced the ‘depleted’ picritic and basaltic eruptions (Jakobsson et al. 1978). The majority of the plotted Reykjanes Peninsula data are from samples younger than <20 ka, and most are post-glacial (i.e. <13 ka), although data from a few sub-glacial eruptions (most likely ~20–100 ka) from Stapafell and the Hengill volcanic system are also plotted

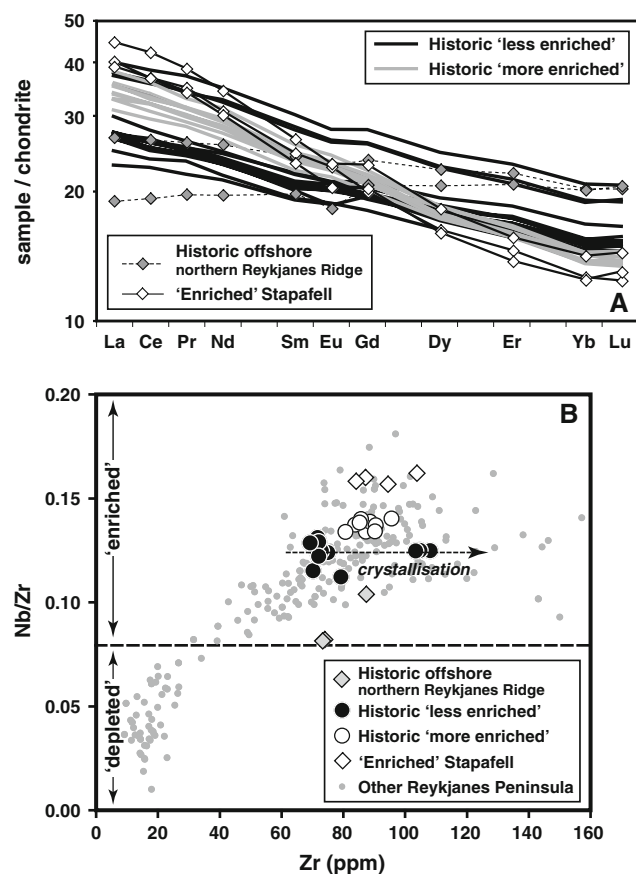


Fig. 4 **a** Chondrite-normalised REE patterns for the historic Reykjanes Peninsula lavas, the historic offshore lavas, and the sub-glacial Stapafell eruption (normalising values from Anders and Grevesse 1989). **b** Zr versus Nb/Zr, to show the relatively restricted range in Nb/Zr of the historic lavas compared to magmatism of the Reykjanes Peninsula as a whole (Hémond et al. 1993; Gurenko and Chaussidon 1995; Gee et al. 1998b, 1999; Révillon et al. 1999; Chauvel and Hémond 2000; Kempton et al. 2000; Hanan et al. 2000; Skovgaard et al. 2001; Kokfelt et al. 2006). These diagrams illustrate the division of the historic lavas into a 'less enriched' group (La/Yb_N 1.3–2.0; Nb/Zr 0.10–0.13) and a 'more enriched' group (La/Yb_N 2.2–2.6; Nb/Zr 0.13–0.14). Boundary between 'enriched' and 'depleted' samples for the Reykjanes Peninsula as a whole is taken from Gee et al. (1998b)

whereas sample 456714 is the only sample analysed for oxygen isotopes that has a significant population of crystals with higher An contents of An_{87} to An_{91} (Fig. 2b).

Discussion

Evidence for two-component mixing in the historic Reykjanes Peninsula lavas

The virtually aphyric nature of the historic lavas means that their compositions approach a true liquid composition. Compositional data demonstrate that the historic lavas do not form a simple cogenetic series of samples that lie on a

single liquid line of descent related by differences in the extent of fractional crystallisation. This is apparent from the range in TiO_2 and K_2O contents at a given MgO content (Fig. 3) and from the range in incompatible trace element ratios such as Nb/Zr and La/Yb (Fig. 4). Given the limited variation in $^{87}\text{Sr}/^{86}\text{Sr}$ (0.70309–0.70314) and ϵNd (+7.3 to +7.8), it is tempting to explain the range in incompatible trace element ratios simply through differences in the melt generation process involving a homogeneous mantle source, but this can be dismissed because of the significant Pb isotope variations revealed with the high precision (double-spike) data (Fig. 6).

A striking feature of the historic lavas are the coherent linear trends shown by high-precision Pb isotope data. All samples plot within analytical uncertainty (± 150 ppm external reproducibility) of a least-squares linear regression line on plots of $^{206}\text{Pb}/^{204}\text{Pb}$ versus $^{207}\text{Pb}/^{204}\text{Pb}$ and $^{208}\text{Pb}/^{204}\text{Pb}$ (Fig. 6b, d), except for sample 456723 which lies about 300 ppm off the $^{206}\text{Pb}/^{204}\text{Pb}$ versus $^{208}\text{Pb}/^{204}\text{Pb}$ trend line. Similar trends in high-precision Pb isotope data have been reported in other ocean island settings (e.g. Hawaii—Abouchami et al. 2000; Eisele et al. 2003; Pitcairn—Eisele et al. 2002; Samoa—Workman et al. 2004), and in each case these trends have been interpreted as binary mixing arrays between compositionally distinct components in the mantle rather than as mantle isochrons, based on correlations with other isotope and elemental ratios. According to Abouchami et al. (2000), whether or not linear Pb isotope arrays represent isochrons or mixing lines can be evaluated by comparing κ ($^{232}\text{Th}/^{238}\text{U}$ inferred from Pb isotopes) with κ^* ($^{232}\text{Th}/^{238}\text{U}$ calculated from Th and U contents): if κ and κ^* are significantly different, then the Pb isotope arrays are unlikely to be isochrons. For the historic Reykjanes Peninsula lavas, κ and κ^* are calculated using the procedure outlined by Abouchami et al. (2000). κ is calculated to be ~ 2.3 from the slopes of the arrays on the $^{206}\text{Pb}/^{204}\text{Pb}$ – $^{207}\text{Pb}/^{204}\text{Pb}$ and $^{206}\text{Pb}/^{204}\text{Pb}$ – $^{208}\text{Pb}/^{204}\text{Pb}$ plots, while $\kappa^* = 3.12 \pm 0.02$ based on six isotope dilution Th and U concentration measurements (Peate et al. 2001; Kokfelt et al. 2003), and this difference is more consistent with a binary mixing origin.

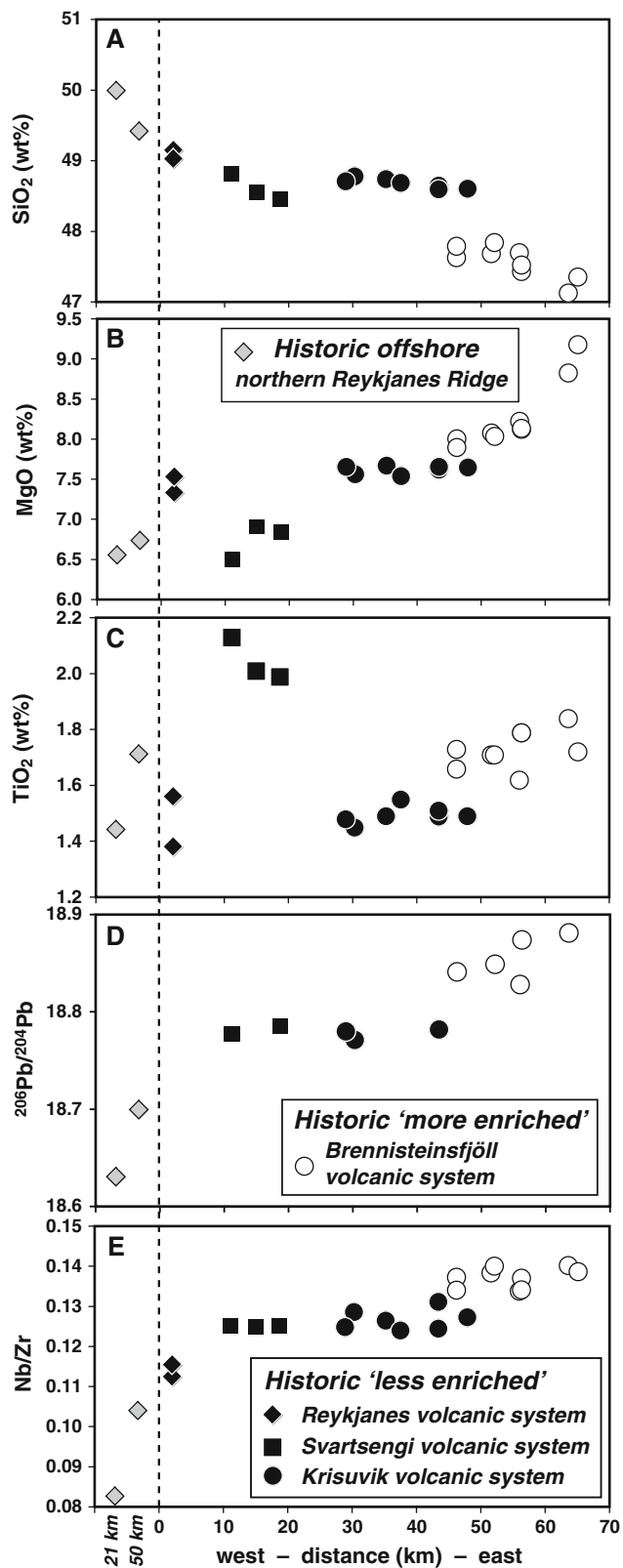
The observed range in $^{143}\text{Nd}/^{144}\text{Nd}$ for historic Reykjanes Peninsula magmas is 0.000017 (0.513014–0.513031; Fig. 5e), which is about two times the typical external precision of the $^{143}\text{Nd}/^{144}\text{Nd}$ measurement (2 SD of 0.000010; e.g. Thirlwall et al. 2004). This compares with the range in $^{206}\text{Pb}/^{204}\text{Pb}$ of 0.11 (18.771–18.881; Fig. 6a), which is greater than 40 times the typical external precision of the double-spike $^{206}\text{Pb}/^{204}\text{Pb}$ measurement (2 SD of <0.003 ; e.g. Thirlwall et al. 2004; Baker et al. 2004). This highlights the advantages of high-precision Pb isotope data to resolve evidence for fine-scale mixing processes (see also Abouchami et al. 2000).

Fig. 5 Spatial compositional variations in the historic Reykjanes Peninsula lavas: **a** SiO₂, **b** MgO, **c** TiO₂, **d** ²⁰⁶Pb/²⁰⁴Pb, **e** Nb/Zr. The horizontal axis is the distance of the eruptive fissure for each sampled flow, projected onto a ENE line from the SW tip of the Reykjanes Peninsula to Hengill. The two offshore samples are plotted at arbitrary distances (see Fig. 1c)

On a plot of La/Yb_N versus Dy/Yb_N (where *N* indicates chondrite normalised ratio: Fig. 7a), binary mixing will produce a linear array, and the historic lavas all plot within the analytical reproducibility (estimated at $\pm 1.5\%$, 2 SD) of a linear regression line through the data. This contrasts with the strongly curved arrays expected for melting: for example, Fig. 7d shows the hyperbolic trajectory of instantaneous fractional melt compositions from the melting model of Maclennan et al. (2003a) for rift zone tholeiites in the Northern Volcanic Zone of Iceland. The broad correlation of incompatible element ratios (e.g. La/Yb_N) with Pb isotope ratios (Fig. 7c) provides additional evidence for binary mixing between a ‘depleted’ end-member with ²⁰⁶Pb/²⁰⁴Pb <18.7 and La/Yb_N <1.3 and an ‘enriched’ end-member with ²⁰⁶Pb/²⁰⁴Pb > 18.9 and La/Yb_N > 2.7.

If the linear array on the La/Yb_N versus Dy/Yb_N plot was the result of magma mixing just prior to eruption, then the data should also form a linear array on a plot of La/Yb_N versus 1/Yb. However, Fig. 7b shows that this is not the case, and in general the variations of incompatible element ratios and Pb isotope ratios do not correlate with elemental abundances in the historic lavas. This implies that the mixing must have occurred prior to variable extents of fractional crystallisation. Additional information as to the timing of mixing relative to crystallisation can potentially be obtained from melt inclusions in olivines. Olivine-hosted melt inclusions in samples from elsewhere in Iceland show a wide compositional range, attesting to the presence of compositionally diverse melts concomitant with olivine growth (e.g. Gurenko and Chaussidon 1995; Maclennan et al. 2003b). Furthermore, Maclennan et al. (2003b) showed that for the Borgarhraun flow in NE Iceland, the variability of REE compositions in the melt inclusions decreased as the Fo content of the host olivine crystal decreased, consistent with progressive mixing taking place concurrently with the early stages of crystallisation.

Figure 7d shows that there is a large compositional diversity of melts potentially available within a melt column from mixing between different instantaneous melts, and yet spatially and temporally restricted suites of basaltic lavas, like the historic Reykjanes Peninsula lavas, often show evidence for binary mixing between two compositionally restricted end-members. Maclennan (2008) has argued that this might be a natural consequence of the melt transport network involving channelised porous flow as envisaged by Spiegelman and Kelemen (2003). Melt travelling in the



channel centres will be relatively ‘enriched’ in incompatible trace elements and generated over the full depth range of the melt column, while melts in the channel margins are

Table 3 High-precision double-spike Pb isotope data for Reykjanes Peninsula lavas

Sample	Flow	$^{206}\text{Pb}/^{204}\text{Pb}$	$^{207}\text{Pb}/^{204}\text{Pb}$	$^{208}\text{Pb}/^{204}\text{Pb}$
Historic offshore lavas (northern Reykjanes Ridge)				
NI-3605	Eldeyjarbodi	18.699	15.503	38.321
NI-13958	Steinaholl	18.630	15.486	38.215
Historic 'less enriched' Reykjanes Peninsula lavas				
Svartsengi volcanic system				
408673	Eldvarpahraun	18.777	15.508	38.394
456722	Arnarseturshraun	18.785	15.508	38.400
Krisuvik volcanic system				
456723	Afstaparhraun yngra	18.771	15.505	38.377
456746	Kapelluhraun	18.782	15.509	38.396
408666	Ögmundarhraun	18.780	15.509	38.395
RP65 N ^a	Ögmundarhraun (Thirlwall)	18.786	15.509	38.403
Historic 'more enriched' Reykjanes Peninsula lavas				
Brennisteinsfjöll volcanic system				
456733	Breiddalshraun	18.841	15.512	38.431
456743	Tvibollahraun	18.849	15.513	38.439
456742	Rjupnadyngnahraun	18.828	15.513	38.430
456740	Kongsfellshraun	18.874	15.517	38.459
456737	Svinahraun sydra	18.881	15.514	38.458
Stapafell subglacial lava (~20–100 ka)—'enriched' Reykjanes Peninsula lava				
456712	Stapafell	18.883	15.516	38.474
456749	Stapafell	18.895	15.518	38.486
sk89-29c ^b	Stapafell	18.887	15.515	38.474
Ice3 ^d	Stapafell	18.887	15.511	38.467
Stapafell	Mean ($n = 4$)	18.888	15.515	38.475
	2 SD	0.010	0.006	0.016
RP67E ^a	Stapafell (Thirlwall)	18.886	15.517	38.480
Other post-glacial (<13 ka) Reykjanes Peninsula lavas				
9805 ^d	Haleyjabunga	18.299	15.472	38.045
207901 ^c	Haleyjabunga	18.295	15.477	38.049
456751	Haleyjabunga	18.297	15.480	38.061
RP80D ^a	Haleyjabunga (Thirlwall)	18.287	15.483	38.059
D2/11 ^a	Haleyjabunga (Thirlwall)	18.305	15.485	38.067
408672 ^c	Lagafell(?)	18.301	15.477	38.045
Ice2 ^d	Lagafell	18.499	15.468	38.133
D7	Lagafell	18.476	15.468	38.118
RP95C ^a	Lagafell	18.480	15.468	38.122
208224 ^c	Asar	18.480	15.494	38.162
208222 ^c	Vatnsheidi	18.577	15.498	38.271
D26 ^c	Burfell	18.449	15.491	38.190
208225 ^c	Dimmidalur (near Hengill)	18.583	15.511	38.213
D18	Hlidarhraun	18.370	15.484	38.138
408669 D1	Skalafell	18.692	15.497	38.307

Pb isotope analyses were done on hand-picked rock chips, leached in 6 M HCl on a hot plate for ~2 h. Samples were analysed using a ^{207}Pb – ^{204}Pb double spike to control mass fractionation, following the procedures outlined in Baker et al. (2004). Measurements were made on a VG Axiom MC–ICP–MS at the Danish Lithosphere Centre, Copenhagen. We measured $^{206}\text{Pb}/^{204}\text{Pb}$ 16.9419 ± 19 , $^{207}\text{Pb}/^{204}\text{Pb}$ 15.4997 ± 22 and $^{208}\text{Pb}/^{204}\text{Pb}$ 36.7246 ± 61 for the SRM981 Pb standard (2 SD, $n = 5$). Total procedural blank was ~80 pg Pb. New double-spike analyses of Reykjanes Peninsula samples from Kurz et al. (1985), Skovgaard et al. (2001) and Brandon et al. (2007) are also included: these samples are all post-glacial in age, except for sk89-29c from the subglacial Stapafell eruption (~20–100 ka). External reproducibility is larger than the internal precision (see Baker et al. 2004). Although Skovgaard et al. (2001) say that 408672 is from Lagafell, it has a Pb isotope composition identical to Haleyjabunga

^a Analyses on samples of the same flows from Thirlwall et al. (2004), for comparison.

^b Kurz et al. (1985)

^c Skovgaard et al. (2001)

^d Brandon et al. (2007)

Table 4 Sr–Nd–O isotope data for Reykjanes Peninsula lavas

Sample	$^{87}\text{Sr}/^{86}\text{Sr}$ Measured	$^{143}\text{Nd}/^{144}\text{Nd}$ Measured	$\delta^{18}\text{O}$ Olivine ‰ (V-SMOW)	$\delta^{18}\text{O}$ Plag ‰ (V-SMOW)	$\Delta^{18}\text{O}_{\text{pl-ol}}$
Historic offshore lavas (northern Reykjanes Ridge)					
NI-3605	–	0.513039	–	–	–
NI-13958	–	0.513077	–	–	–
Historic ‘less enriched’ Reykjanes Peninsula lavas					
Reykjanes volcanic system					
456714	0.703093	0.513031	4.22	5.40, 5.58	1.18, 1.36
456716	–	0.513029	–	–	–
Svartsengi volcanic system					
408673	0.703118	0.513031	–	–	–
456722	–	0.513021	–	–	–
Krisuvik volcanic system					
456723	0.703106	0.513019	–	–	–
456746	0.703122	0.513014	–	5.13	–
408666	0.703119	0.513018	–	–	–
Historic ‘more enriched’ Reykjanes Peninsula lavas					
Brennisteinsfjöll volcanic system					
456733	0.703134	0.513020	4.20	5.10	0.90
456743	0.703138	0.513015	–	–	–
456742	–	0.513031	4.33	5.03	0.70
456740	0.703120	0.513024	–	–	–
456737	0.703130	0.513023	4.21	–	–
Stapafell subglacial lava (~20–100 ka)—‘enriched’ Reykjanes Peninsula lava					
456712	–	0.512998	–	–	–
456749	0.703166	0.513001	4.77	–	–
Other post-glacial (<13 ka) Reykjanes Peninsula lavas					
408672	–	0.513092	5.15	–	–

Sr–Nd–O isotope data for Reykjanes Peninsula lavas. All Sr–Nd isotope analyses were measured on a VG Axiom MC–ICP–MS at the Danish Lithosphere Centre, Copenhagen. Sr and Nd isotopes were determined on powders, leached in 6 M HCl on a hot plate for ~2 h. The analytical procedures for chemical separation and mass spectrometry are detailed in Peate et al. (2003) and Waight et al. (2002). The SRM987 Sr standard gave 0.710248 ± 15 (2 SD, $n = 10$), and the $^{87}\text{Sr}/^{86}\text{Sr}$ data are presented relative to 0.71025 for SRM987. The Ames Nd metal (plus admixed Sm metal) standard gave 0.512128 ± 7 , and the $^{143}\text{Nd}/^{144}\text{Nd}$ data are presented relative to an Ames Nd metal standard value of 0.51213. An analysis of BHVO-1 gave $^{143}\text{Nd}/^{144}\text{Nd} = 0.512983$. The internal precision on individual $^{87}\text{Sr}/^{86}\text{Sr}$ and $^{143}\text{Nd}/^{144}\text{Nd}$ analyses are less than the external reproducibility of replicate analyses. Oxygen isotope data were obtained at Royal Holloway University of London using a LaserPrep system on line to a VG Optima dual inlet mass spectrometer (Mattey and Macpherson 1993; Thirlwall et al. 2006). Aliquots of pure mineral separates (1.7 mg) were combusted via a Synrad CO₂ laser in the presence of excess BF₅. The San Carlos Olivine II standard gave $\delta^{18}\text{O}$ of $5.24 \pm 0.09\text{‰}$ ($n = 11$), and the GMG II standard gave $\delta^{18}\text{O}$ of $5.72 \pm 0.03\text{‰}$ ($n = 5$), which are calibrated against the NBS-30 biotite at $+5.1\text{‰}$. All $\delta^{18}\text{O}$ values are reported relative to V-SMOW. The overall precision on standards and sample replicates is better than $\pm 0.1\text{‰}$.

generated in the shallowest mantle and have strongly ‘depleted’ incompatible trace element contents. Mixing between the channel centre and channel margin melts in magma bodies at the top of the melt column can potentially lead to the binary mixing arrays seen in both the whole rock samples and in olivine-hosted melt inclusions.

Fractional crystallisation within the historic Reykjanes Peninsula lavas

Jakobsson et al. (1978) summarised the main petrographic features of the post-glacial Reykjanes tholeiitic lava shield

and fissure lavas. For lavas with $\text{FeO}^*/\text{MgO} < \sim 1.4$, olivine is the sole phenocryst phase, while lavas with $\text{FeO}^*/\text{MgO} > \sim 1.4$ have both olivine and plagioclase phenocrysts, with minor amounts of clinopyroxene. The historic lavas conform to this pattern, as all the flows (except the Svinahraun flows) contain both olivine and plagioclase phenocrysts. The Svinahraun flows, which belong to the ‘more enriched’ group from the Brennisteinsfjöll volcanic system, have the lowest FeO^*/MgO (~ 1.3) and contain only olivine phenocrysts. The effects of plagioclase crystallisation are apparent as resolvable negative Eu-anomalies (Fig. 4) in samples with FeO^*/MgO

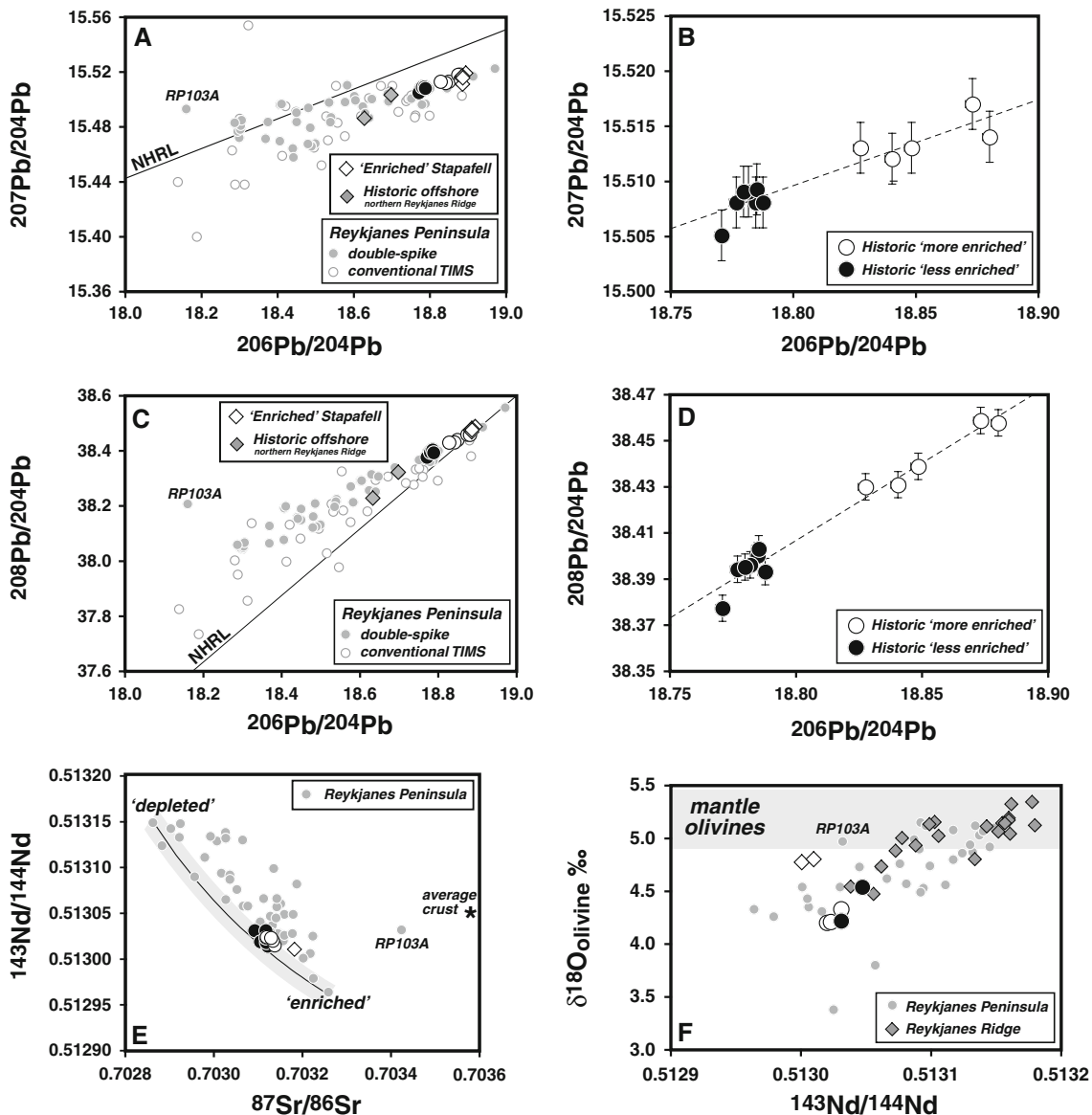


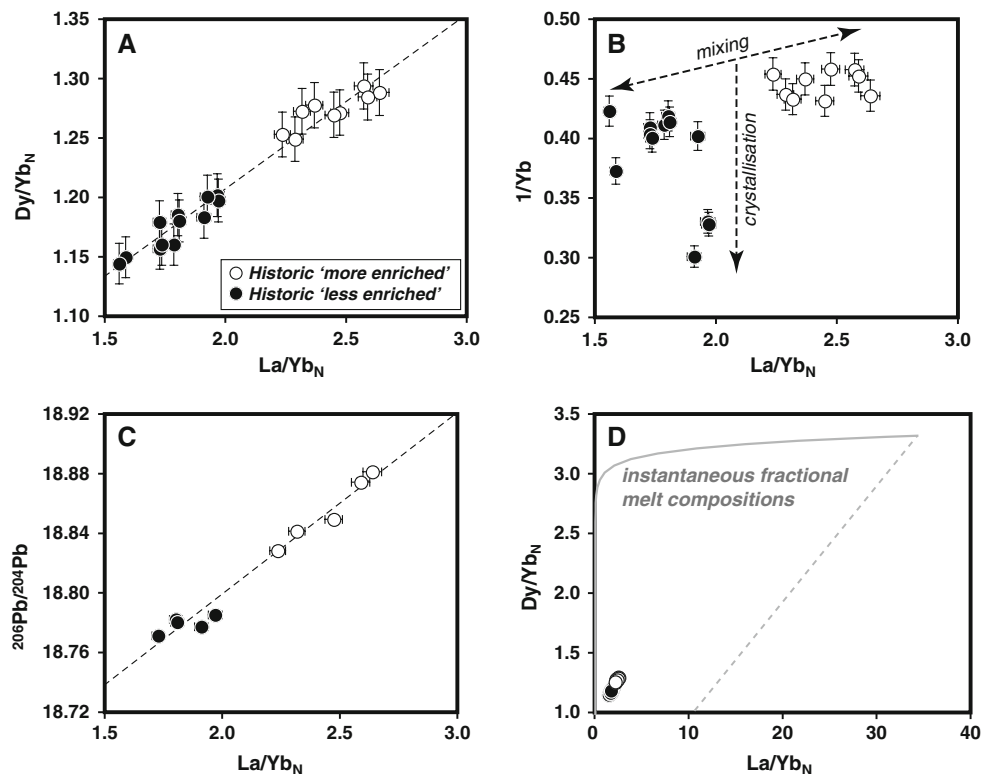
Fig. 6 Isotope variations within the historic lavas: **a**, **b** $^{206}\text{Pb}/^{204}\text{Pb}$ versus $^{207}\text{Pb}/^{204}\text{Pb}$, **c**, **d** $^{206}\text{Pb}/^{204}\text{Pb}$ versus $^{208}\text{Pb}/^{204}\text{Pb}$, **e** $^{87}\text{Sr}/^{86}\text{Sr}$ versus $^{143}\text{Nd}/^{144}\text{Nd}$, **f** $\delta^{18}\text{O}_{\text{olivine}}$ versus $^{143}\text{Nd}/^{144}\text{Nd}$. Data for other Reykjanes Peninsula lavas are shown for comparison (Sun and Jahn 1975; Condomines et al. 1983; Elliott et al. 1991; Hémond et al. 1993; Hanan and Schilling 1997; Gee et al. 1998b; Kempton et al. 2000; Chauvel and Hémond 2000; Skovgaard et al. 2001; Thirlwall et al. 2004, 2006; Blichert-Toft et al. 2005; Kokfelt et al. 2006; Tables 3, 4). These other Reykjanes Peninsula samples are all post-glacial (<13 ka) except for three samples from Thirlwall et al. (2004, 2006) that are 13–20 ka. Error bars plotted on (b) and (d) are ± 150 ppm 2 SD external reproducibility, and the dotted lines are a least-squares linear regression line through the data. On (e), the black line represents a hypothetical mixing curve between 'depleted' and 'enriched' melts

(samples RP95C and RP100C, respectively: Thirlwall et al. 2004), and the grey shaded area represents the estimated analytical uncertainty ($\sim \pm 20$ ppm, 2 SD). Estimate of average composition of Reykjanes Peninsula hydrothermally altered crust ($^{87}\text{Sr}/^{86}\text{Sr} = 0.7036$, $^{143}\text{Nd}/^{144}\text{Nd} = 0.51305$, $\delta^{18}\text{O}_{\text{olivine}} = +2\text{‰}$) from Gee et al. (1998b). RP103A is a sample from Kleifarvatn that Thirlwall et al. (2004) use to define their ID2 component. NHRL is the Northern Hemisphere Reference Line (from Hart 1984). For some Reykjanes Ridge samples in (f), $\delta^{18}\text{O}_{\text{olivine}}$ was calculated from $\delta^{18}\text{O}_{\text{glass}}$ assuming an olivine-melt fractionation factor of $+0.4\text{‰}$ (e.g. Eiler 2001). Note that the plotted $\delta^{18}\text{O}_{\text{olivine}}$ values are measured on ~ 2 –10 grains, which will average out any potential within-sample heterogeneity that has been demonstrated in olivines from some mafic lavas elsewhere in Iceland (e.g. MacLennan et al. 2003b; Bindeman et al. 2006)

>1.6 (equivalent to MgO <7.5 wt%). These evolved samples have Eu/Eu* values of 0.94–0.98, while the more primitive higher MgO and lower FeO*/MgO samples have Eu/Eu* values of 0.98–1.03. Crystallisation temperatures

were estimated using the olivine-liquid thermometer of Putirka (1997). Not all of the analysed olivine crystals are in equilibrium with their host melt, based on Fe–Mg partitioning (Fig. 2b), and so only those olivines that had

Fig. 7 **a** La/Yb_N versus Dy/Yb_N , **b** La/Yb_N versus $1/\text{Yb}$, **c** La/Yb_N versus $^{206}\text{Pb}/^{204}\text{Pb}$, for the historic Reykjanes Peninsula lavas. Dotted lines in (a) and (c) are least-squares linear regression lines through the data. The absence of a linear trend shown by the data in (b) indicates that variable extents of crystallisation occurred subsequent to mixing. (d) plot showing the strong curvature of melting models for La/Yb_N versus Dy/Yb_N ; the solid grey line shows the path of instantaneous fractional melt compositions from the melting model of MacLennan et al. (2003a), and compositions that can be generated by mixing of the fractional melts will lie between the solid and dotted grey lines



measured $K_{D(\text{Fe}-\text{Mg})}$ within the expected range for samples of these lava compositions (0.25–0.36; Putirka 2005) were used for temperature calculations. The data indicate that olivine crystallisation in the historic lavas took place at temperatures between $\sim 1,180^\circ\text{C}$ and $\sim 1,200^\circ\text{C}$, $\sim 15^\circ\text{C}$ lower than the experimentally determined 1 atm. liquidus (Fisk et al. 1980), which is within the $\pm 31^\circ\text{C}$ calibration error estimated by Putirka (1997) for this thermometer.

Although geobarometers such as Putirka et al. (1996) and Nimis and Ulmer (1998) can potentially provide estimates of the pressure of clinopyroxene crystallisation, their applicability is limited because clinopyroxene is not a common phenocryst phase in the historic Reykjanes Peninsula lavas. Clinopyroxene was only analysed in two samples of the 'less enriched' group. The Putirka et al. (1996) model requires equilibrium melt-clinopyroxene pairs, and this can be assessed using Fe–Mg partitioning. The equations in Putirka et al. (1996) were used to calculate expected $K_{D(\text{Fe}-\text{Mg})}$ values of 0.33 ± 0.01 for these two melt compositions. Disequilibrium between these clinopyroxenes and their host melts is indicated by the significantly lower measured $K_{D(\text{Fe}-\text{Mg})}$ values (0.24 ± 0.02). However, the Nimis and Ulmer (1998) geobarometer estimates pressure from just the clinopyroxene composition: sample 456746 gives pressures of 0.21 ± 0.05 GPa and sample 456714 gives pressures of 0.53 ± 0.10 GPa. These are equivalent to crystallisation depths of $\sim 7 \pm 2$ and $\sim 18 \pm 4$ km, respectively.

Pressures of crystallisation can also be estimated by comparing sample compositions with experimentally determined ol–plag–cpx cotectic melt compositions. This requires that sample analyses represent liquid compositions, which is a reasonable assumption given the virtually aphyric nature of the historic flows, and also that the melts were in equilibrium with olivine + plagioclase + clinopyroxene. This latter requirement is more difficult to establish unequivocally, given the limited range in MgO within each volcanic system (Fig. 5). The 'less enriched' flows show a general trend of decreasing CaO and Ca/Al with decreasing MgO, consistent with cotectic crystallisation. Although clinopyroxene was only found in trace amounts in flows of the 'less enriched' group, the absence of more abundant cpx phenocrysts in these flows may be due to resorption during ascent. The model of Kelley and Barton (2008) was used to estimate pressures of crystallisation (to ± 0.1 GPa accuracy) for the historic flows, grouped according to volcanic system (Fig. 1): Reykjanes volcanic system, 0.34–0.39 GPa ($n = 2$); Svartsengi volcanic system, 0.46–0.50 GPa ($n = 3$); Krisuvik volcanic system, 0.33–0.37 GPa ($n = 7$); Brennisteinsfjöll volcanic system (excluding the Svinahraun flows), 0.60–0.72 GPa ($n = 7$). For the 'less enriched' group, flows from the Reykjanes and Krisuvik volcanic systems have similar crystallisation depths of ~ 11 – 14 km, while the flows from the Svartsengi volcanic system give deeper calculated crystallisation depths of ~ 16 – 18 km. The crustal thickness

along the Reykjanes Peninsula is 15–18 km (Weir et al. 2001), and so these data, together with the limited clinopyroxene geobarometry suggest that crystallisation in the historic lavas has taken place over a range of depths within the crust. This is consistent with observations at other locations in the Reykjanes Peninsula and elsewhere in Iceland (see summary in Kelley and Barton 2008). The sub-Moho crystallisation depths (~ 21 – 26 km) inferred for the ‘*more enriched*’ lavas from the Brennisteinsfjöll volcanic system are more likely an artifact of these samples crystallising just ol + plag rather than the cotectic ol–plag–cpx assemblage, as they show a trend of increasing CaO and Ca/Al with decreasing MgO.

The ‘*less enriched*’ group (except Stampahraun) has a limited range in incompatible element ratios (e.g. Nb/Zr Figs. 4b, 5e) and Pb isotope ratios (Figs. 5d, 6), and so they might be expected to fall on a simple liquid line of descent as MgO decreases from 7.7 to 6.5 wt%, but this is not the case. The lavas from the Krisuvik Fires episode (1151–1188 AD), together with the Eldborgarhraun and Afstapahraun flows from the same volcanic system (that have slightly younger inferred ages ~ 1325 AD), have remarkably similar compositions and share some distinctive characteristics that distinguish them from the other flows in the ‘*less enriched*’ group, such as high Ca/Al. Although samples from the adjacent Svartsengi volcanic system have more evolved compositions, they have similar or higher Cr values (124–175 ppm) compared to the flows in the Krisuvik volcanic system (111–149 ppm), but lower Ni contents (65–74 vs. 81–89 ppm). Furthermore, there are small but significant differences in Ba/Nb, two highly incompatible trace elements (Svartsengi volcanic system 4.6–5.0 vs. Krisuvik volcanic system 5.9–6.5). Therefore, the history of mantle-derived melts of similar composition must vary in detail between the different volcanic systems along the length of the Reykjanes Peninsula, as a result of subtle differences in the melt transport regime, depths of crystallisation within the crust, and in the extent of interaction with crustal materials (assimilation and melt percolation through gabbroic cumulates: e.g. Gurenko and Sobolev 2006).

‘Enriched’ and ‘depleted’ mantle components on the Reykjanes Peninsula

Recent (<20 ka) magmatism on the Reykjanes Peninsula shows a far greater compositional diversity compared to the historic lavas (Figs. 3, 4b, 6). This variability is shown in petrography, major and trace elements, and isotopes (e.g. Jakobsson et al. 1978; Zindler et al. 1979; Elliott et al. 1991; Gee et al. 1998b; Thirlwall et al. 2004, 2006; Kokfelt et al. 2006). Several authors have suggested that a dynamic melting model could account for much of the observed

compositional diversity of melt compositions, at length scales ranging from whole rock samples (e.g. Wood 1981; Elliott et al. 1991) down to olivine-hosted melt inclusions (Gurenko and Chaussidon 1995). Deep melts derived from the base of the melting column will have high Fe and will be enriched in incompatible trace elements. In contrast, shallow melts from the top of the melting column will have low Fe and they will also be depleted in incompatible trace elements as these elements will have been largely removed from the mantle at deeper levels in the melting column. However, the range in Sr–Nd–Pb isotopic compositions in the lavas requires a compositionally heterogeneous source in which the most incompatible element depleted samples (e.g. Nb/Zr ~ 0.01 ; La/Yb_N ~ 0.2) are derived from a time-integrated depleted source (high $^{143}\text{Nd}/^{144}\text{Nd} \sim 0.51316$). Therefore, a model involving polybaric melting of a heterogeneous mantle comprised of enriched streaks set in a refractory depleted matrix is the preferred solution of many workers (e.g. Chauvel and Hémond 2000; Fitton et al. 2003; Stracke et al. 2003; Kokfelt et al. 2006). This is consistent with recent olivine-hosted melt inclusion data that preserve, in a single lava sample, the full Pb isotopic range of all Reykjanes Peninsula lavas (Maclennan 2008).

The isotopic variability of recent (<20 ka) Reykjanes Peninsula lavas can be broadly explained by mixing between a ‘*depleted*’ component with $^{87}\text{Sr}/^{86}\text{Sr} \sim 0.70286$, $^{143}\text{Nd}/^{144}\text{Nd} \sim 0.51316$ and $^{206}\text{Pb}/^{204}\text{Pb} \sim 18.25$, and an ‘*enriched*’ component with $^{87}\text{Sr}/^{86}\text{Sr} \sim 0.70326$, $^{143}\text{Nd}/^{144}\text{Nd} \sim 0.51296$ and $^{206}\text{Pb}/^{204}\text{Pb} \sim 18.95$ (e.g. Stecher et al. 1986; Gee et al. 1998b; Thirlwall et al. 2004, 2006; this paper). The incompatible element concentrations of the two end-members differ by about an order of magnitude (e.g. Fig. 4b; Gee et al. 1998b), and this marked difference can explain the lack of variation in the Sr and Nd isotope composition of the historic lavas. Simple binary mixing models (Langmuir et al. 1978), using samples from Thirlwall et al. (2004) as representative of the two end-members (‘*depleted*’ RP95C; ‘*enriched*’ RP100C), indicate that the restricted range in the Sr and Nd isotope compositions of historic lavas can in fact accommodate a broad range of mixtures involving between 50 and 90% of the ‘*enriched*’ end-member. The ‘*depleted*’ end-member is only found in a relatively undiluted form in the small-volume picrites erupted during the last deglaciation (9–13 ka: e.g. Jakobsson et al. 1978).

Post-glacial magmatism on the Reykjanes Peninsula is actually dominated by lavas with ‘*enriched*’ compositions (i.e. Nb/Zr >0.08 ; La/Yb_N >1.0) similar to the historic lavas. For example, Thirlwall et al. (2006) noted that the average Nb/Zr was 0.130 for their suite of 253 samples. Jakobsson et al. (1978) estimated the volumes of the various eruptive units found in the western half of the Reykjanes Peninsula and showed that the ‘*depleted*’

picritic lavas are volumetrically negligible (less than 2% of the total volume). The two main lava shields (Sandfells-haed and Thrainsskjöldur: Fig. 1), which were erupted shortly after the deglaciation interval that produced the ‘depleted’ picritic and basaltic eruptions, comprise about two-thirds of total volume of post-glacial magmas erupted on the Reykjanes Peninsula and these lavas have ‘enriched’ compositions (Fig. 3: Jakobsson et al. 1978), with $\text{La}/\text{Yb}_N > 1.3$ (Zindler et al. 1979).

An intriguing feature of the historic Reykjanes Peninsula lavas is the systematic geographical compositional variation (Fig. 5). Historic lavas erupted from individual volcanic systems have broadly similar compositions, but differ from those in the adjacent volcanic systems. The main geographical trend is one of decreasing trace element enrichment, best shown by the east to west decrease in Nb/Zr that continues in the offshore historic lavas of the northern Reykjanes Ridge (Fig. 5e). While it is tempting to attribute this to a systematic spatial compositional variation in the mantle source beneath the Reykjanes Peninsula, it is important to remember that the historic lavas represent a relatively short time period of magmatic activity (~400 years). In fact, over the last 9,000 years, each of the volcanic systems has erupted lavas that span the full range in Nb/Zr seen in the historic lavas (e.g. Gee et al. 2000). Therefore, the lateral gradient in Nb/Zr shown by the historic lavas along the Reykjanes Peninsula is more likely to be just a coincidence, with the Nb/Zr variations reflecting a complex interplay between the scale of mantle compositional heterogeneity, the footprint of the melt generation zone, and the progressive tapping of melts from this zone. However, the trend of decreasing SiO_2 from west to east is part of a longer wavelength variations that continues offshore to the south-west along the northern Reykjanes Ridge and to the north-east along the Western Volcanic Zone (e.g. Jakobsson et al. 2000). SiO_2 contents of primitive mafic melts are influenced by the depth of melting as well as source mineralogy. The gradual lateral change in SiO_2 therefore might simply reflect an increase in the average depth of melting in response to elevated mantle temperatures and/or more active plume-driven upwelling closer to the center of Iceland, consistent with U-series disequilibrium data (Peate et al. 2001; Kokfelt et al. 2003).

Pb isotope variations in post-glacial (<13 ka) Reykjanes Peninsula lavas

Thirlwall et al. (2004) presented a comprehensive study of high precision Sr–Nd–Pb isotope variations in volcanic rocks from the main rift zones of Iceland and in the adjacent mid-ocean ridges, and they proposed that these data could be explained by the presence of four major compositionally distinct components within the Icelandic mantle

(ID1, ID2, IE1, IE2). They noted that samples from geographically restricted locations showed tight isotopic correlations consistent with binary mixing, and that in each region the four mantle components can be mixed in various proportions to provide these local mixing end-members. In their model, the ‘enriched’ component of the Reykjanes Peninsula is composed of a well-blended mixture of IE1 + IE2 and this mixture then variably mixes with the ‘depleted’ component ID1 to form the observed data array (Fig. 8). A minor influence from the ID2 component was required to account for the rare Reykjanes Peninsula samples with positive $\Delta^{207}\text{Pb}$.

The new high-precision Pb isotope data (Table 3) for the Reykjanes Peninsula lavas are shown on Fig. 8, together with the high-precision Pb isotope data of Thirlwall et al. (2004), and the compositions of their four inferred mantle components are marked with star symbols. These figures highlight the good agreement between these two independent data sets. On the $^{208}\text{Pb}/^{204}\text{Pb}$ versus $^{206}\text{Pb}/^{204}\text{Pb}$ plot (Fig. 8b), the Reykjanes Peninsula data form a good linear trend that is consistent with an extrapolation to lower $^{206}\text{Pb}/^{204}\text{Pb}$ values of the trend shown by the historic lavas. On the $^{207}\text{Pb}/^{204}\text{Pb}$ versus $^{206}\text{Pb}/^{204}\text{Pb}$ plot (Fig. 8a), the Reykjanes Peninsula data trend becomes increasingly more scattered at low $^{206}\text{Pb}/^{204}\text{Pb}$ values in the trace-element-depleted picritic lavas. Despite the very low Pb contents in these samples (<0.1 ppm; Chauvel and Hémond 2000; Kokfelt et al. 2006; Nielsen et al. 2007), we do not consider the data to have been compromised by analytical issues. We have previously demonstrated the effectiveness of our leaching and analytical procedures to obtain reproducible Pb isotope data on samples with sub-0.2 ppm Pb contents (Baker et al. 2005). For the ‘depleted’ Reykjanes picrites, the compositional extremes are represented by Haleyjabunga and Lagafell. In each location, replicate whole rock samples of the same units give similar Pb isotope compositions, illustrating the robustness of these observations. In detail, the Haleyjabunga sample have significantly higher $^{207}\text{Pb}/^{204}\text{Pb}$ (~15.479) than the Lagafell samples (~15.467), despite their lower $^{206}\text{Pb}/^{204}\text{Pb}$ (18.30 vs. 18.49). This difference is highlighted on the $^{206}\text{Pb}/^{204}\text{Pb}$ versus $\Delta^{207}\text{Pb}$ plot (Fig. 8c), where $\Delta^{207}\text{Pb}$ represents the vertical deviation ($\times 100$) of a sample from the Northern Hemisphere Reference Line (Hart 1984). The Lagafell samples have negative $\Delta^{207}\text{Pb}$ values similar to the historic lavas (–2 to –3), while the Haleyjabunga samples straddle the NHRL with $\Delta^{207}\text{Pb}$ values of –1 to +1. Figure 8d shows that the Haleyjabunga samples and the Lagafell samples are also not colinear with the historic lavas on a $^{206}\text{Pb}/^{204}\text{Pb}$ versus $\Delta^{208}\text{Pb}$ plot.

These isotopic differences are unlikely to be related to alteration and/or assimilation of crustal rocks as the Reykjanes crustal rocks are expected to have high

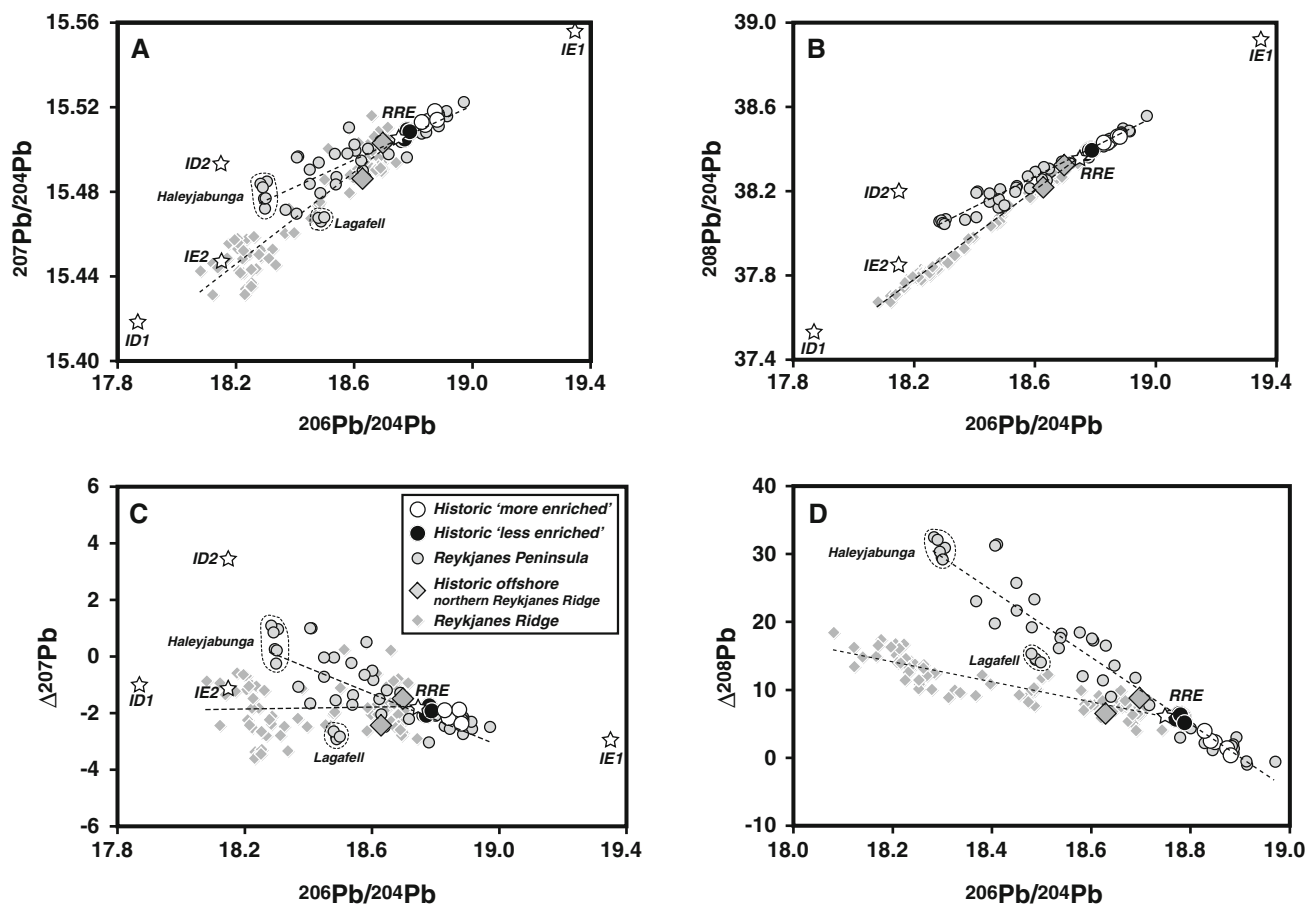


Fig. 8 Regional comparison of Pb isotope compositions of onshore Reykjanes Peninsula lavas and offshore Reykjanes Ridge lavas (this study; Thirlwall et al. 2004; Blichert-Toft et al. 2005). $\Delta^{207}\text{Pb}$ and $\Delta^{208}\text{Pb}$ are the vertical deviations $\times 100$ of samples from the

Northern Hemisphere Reference Line (after Hart 1984). Star symbols are the inferred mixing components that can explain the isotopic variations of Icelandic lavas (ID1, ID2, IE1, IE2) and the RRE component from Thirlwall et al. (2004)

$^{206}\text{Pb}/^{204}\text{Pb}$ (~ 18.8) and fall within the main array of the lavas (see next section). Instead, these data result from isotopic heterogeneity in the mantle and require the presence of at least two components with low $^{206}\text{Pb}/^{204}\text{Pb}$, consistent with the conclusions of Thirlwall et al. (2004). Thirlwall et al. (2004) referred to the component with positive $\Delta^{207}\text{Pb}$ and high $\Delta^{208}\text{Pb}$ as ID2, and its inferred composition was based on replicate analyses of a sample (RP103A) from Kleifarvatn that had an unusual Pb isotope composition (low $^{206}\text{Pb}/^{204}\text{Pb} \sim 18.16$, $\Delta^{207}\text{Pb} \sim 3.4$, $\Delta^{208}\text{Pb} \sim 62$) and enriched Sr–Nd isotope values (Fig. 6e). Based on Fig. 8, it seems that this component has a greater influence on the depleted Reykjanes Peninsula samples than has been previously recognised. The elevated $^{87}\text{Sr}/^{86}\text{Sr}$ value inferred for the ID2 component (>0.70345) might also explain the slightly higher Sr isotope composition of Haleyjabunga compared to Lagafell (0.70302 vs. 0.70289; Hémond et al. 1993; Kokfelt et al. 2006; Thirlwall et al. 2006), despite the lower $^{206}\text{Pb}/^{204}\text{Pb}$ values (see also Thirlwall et al. 2004).

A role for crustal assimilation?

An important issue to resolve is the extent to which shallow-level interaction with the Icelandic crust might have modified the composition of the lavas. Geothermal fluids and hydrothermally altered rocks from the Reykjanes Peninsula have higher $^{87}\text{Sr}/^{86}\text{Sr}$ (0.7037–0.7042; Elderfield and Greaves 1981) than unaltered lavas (<0.7033 ; Fig. 6e) from some seawater input, but $^{143}\text{Nd}/^{144}\text{Nd}$ values are likely to be similar to the average lava composition (e.g. 0.51303–0.51305; Hémond et al. 1993; Gee et al. 1998b) given the limited solubility of Nd in fluids. Therefore, assimilation of hydrothermally altered rocks should produce a shift to elevated $^{87}\text{Sr}/^{86}\text{Sr}$ values (Hémond et al. 1993; Gee et al. 1998b). The historic Reykjanes Peninsula lavas have Sr–Nd isotope compositions that plot within analytical error of a mixing curve between the 'depleted' and 'enriched' mantle components inferred by Stecher et al. (1986) and Gee et al. (1998b), and thus there is no evidence that assimilation of hydrothermally altered crust

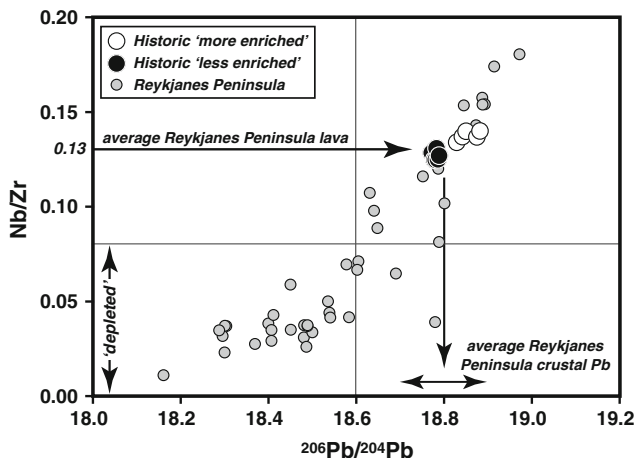


Fig. 9 $^{206}\text{Pb}/^{204}\text{Pb}$ versus Nb/Zr for Reykjanes Peninsula lavas. Data sources: Gee et al. (1998a); Skovgaard et al. (2001); Thirlwall et al. (2004), Nielsen et al. (2007); this study

with elevated $^{87}\text{Sr}/^{86}\text{Sr}$ has noticeably affected the composition of the historic lavas (Fig. 6e). The scatter of published data for other earlier Reykjanes Peninsula lavas can be explained by the assimilation of 5–20% of hydrothermally altered crust by some samples (e.g. Gee et al. 1998b), although some scatter can result from incomplete sample leaching procedures (e.g. Thirlwall et al. 2004) or to the influence of the ID2 mantle component (Fig. 6e).

Crustal assimilation is expected to have a minimal effect on the Pb isotope compositions of the erupted lavas. The average $^{206}\text{Pb}/^{204}\text{Pb}$ ratio of the Reykjanes Peninsula crust can be estimated as $\sim 18.8 \pm 0.1$ from the broad correlation between trace element enrichment/depletion (e.g. Nb/Zr) and $^{206}\text{Pb}/^{204}\text{Pb}$ (Fig. 9), and the average Nb/Zr value of Reykjanes Peninsula lavas of 0.130 (Thirlwall et al. 2004). Its Pb isotope composition should lie within the observed data array of the lavas, because any hydrothermal systems will largely redistribute crustal Pb and the crust is too young for the Pb isotope composition to have significantly changed through radioactive decay. Any assimilation of hydrothermally altered rocks would move Pb isotope compositions along the main array and not perpendicular to it, and therefore could not explain the compositional differences between the different depleted picritic units (e.g. Lagafell vs. Haleyjabunga).

Iceland is notable for the abundance of lavas with $\delta^{18}\text{O}$ values lighter than expected to be in equilibrium with the mantle (e.g. Muehlenbachs et al. 1974; Condomines et al. 1983; Sigmarsson et al. 1992; Hémond et al. 1993; Eiler et al. 2000; Thirlwall et al. 2006), and the historic Reykjanes Peninsula lavas are no exception (Fig. 6f). These lavas have $\delta^{18}\text{O}_{\text{olivine}}$ values of +4.2 to +4.3‰, which are significantly lighter than mean lithospheric mantle olivine compositions ($5.2 \pm 0.3\text{‰}$; Matthey et al. 1994). The origin of this ^{18}O -depleted signature has been the subject of much

debate in the literature over whether it is a feature of the mantle source or acquired through crustal assimilation. Meteoric waters on Iceland have very light $\delta^{18}\text{O}$ due to the high-latitude location of the island, and the extensive hydrothermal systems in the rift zones means that the altered crustal rocks acquire a light $\delta^{18}\text{O}$ signature: strongly altered Reykjanes Peninsula crustal rocks are estimated to have $\delta^{18}\text{O}$ of +2‰ (e.g. Gee et al. 1998a). Bindeman et al. (2006) have suggested that assimilation of palagonitised hyaloclastic volcanic rocks altered by glacial meltwaters might be a suitable mechanism to account for the light $\delta^{18}\text{O}$ values of many Icelandic basalts, such as the 1783 AD Laki eruption, and Pleistocene hyaloclastites near the Laki eruption site had $\delta^{18}\text{O}$ of +2.8 to +3.3‰.

The majority of the Reykjanes Peninsula samples show broad correlations between radiogenic isotopes and oxygen isotopes (e.g. Fig. 6f). The 'depleted' flows with high $^{143}\text{Nd}/^{144}\text{Nd}$, low $^{206}\text{Pb}/^{204}\text{Pb}$ and $\delta^{18}\text{O}$ values similar to normal mantle ($\delta^{18}\text{O}_{\text{olivine}} = +4.9\text{‰}$ to +5.1‰) plot at one end, and the 'enriched' flows with low $^{143}\text{Nd}/^{144}\text{Nd}$, high $^{206}\text{Pb}/^{204}\text{Pb}$ and lighter $\delta^{18}\text{O}$ values plot at the other (Thirlwall et al. 2006). The historic flows anchor the 'enriched' end of the trend with $\delta^{18}\text{O}_{\text{olivine}}$ of +4.2 to +4.3‰. Several studies have noted that olivines within individual samples of Icelandic basalts can have heterogeneous oxygen isotope compositions (e.g. MacLennan et al. 2003b; Bindeman et al. 2006). The Reykjanes Peninsula $\delta^{18}\text{O}_{\text{olivine}}$ data plotted in Fig. 6b are analyses on ~ 2 –10 grains, which will average out any potential within-sample heterogeneity. However, the broad trend shown between these averaged $\delta^{18}\text{O}_{\text{olivine}}$ values and whole-rock $^{143}\text{Nd}/^{144}\text{Nd}$ data require that olivines with light $\delta^{18}\text{O}$ are volumetrically more significant in the 'enriched' low $^{143}\text{Nd}/^{144}\text{Nd}$ flows. Two Reykjanes Peninsula samples have anomalously light $\delta^{18}\text{O}$ (+3.4 to +3.8‰; Fig. 6f) and these samples also have elevated $^{87}\text{Sr}/^{86}\text{Sr}$, consistent with some assimilation of altered crust (e.g. Gee et al. 1998b; Thirlwall et al. 2006).

Thirlwall et al. (2006) showed that some samples from the offshore Reykjanes Ridge also had light $\delta^{18}\text{O}_{\text{olivine}}$ values (down to +4.5‰) and argued, based on curvature of Nd–O mixing arrays and normal Cl/K ratios, that these values represented mantle compositions. This strengthened their arguments that the light $\delta^{18}\text{O}$ in samples from the Reykjanes Peninsula with similar Sr–Nd–Pb isotope compositions were also unaffected by crustal assimilation. Burnard and Harrison (2005) argued that glass samples with high $^{40}\text{Ar}/^{36}\text{Ar}$ ratios ($>2,000$) cannot have been affected by surface alteration or assimilation of altered crust as this would have introduced argon with an atmospheric composition ($^{40}\text{Ar}/^{36}\text{Ar} = 296$). They showed that two samples from Dagmalafell in the Hengill volcanic system of the Reykjanes Peninsula had light $\delta^{18}\text{O}_{\text{glass}}$

values of +4.6‰ (equivalent to $\delta^{18}\text{O}_{\text{olivine}}$ values of $\sim +4.3\text{‰}$) coupled with high $^{40}\text{Ar}/^{36}\text{Ar}$ ratios (4,900–6,500), which indicates that the mantle source had light $\delta^{18}\text{O}_{\text{olivine}}$ of $\sim +4.3\text{‰}$. Thus, it is reasonable to suggest that the light $\delta^{18}\text{O}_{\text{olivine}}$ of the historic lavas represent mantle values, although it is difficult to categorically rule out any role for assimilation. An assessment of within-sample $\delta^{18}\text{O}$ heterogeneity through a detailed study of individual olivine crystals might help to resolve this issue (e.g. Bindeman et al. 2006). Another approach would be to look at melt inclusions in olivine and plagioclase crystals to see if there is any evidence for elevated chlorine abundances that should be an unequivocal tracer for the assimilation of crustal lithologies hydrothermally altered by fluids of seawater origin (e.g. Kent et al. 1999). While hydrothermal systems across Iceland are mostly dominated by meteoric water, the active systems in the south-eastern part of the Reykjanes Peninsula (e.g. Reykjanes, Svartsengi) are dominated by seawater flow that should introduce significant quantities of chlorine into the altered crustal lithologies (e.g. Kadko et al. 2007).

Comparison of onshore Reykjanes Peninsula lavas and offshore Reykjanes Ridge lavas

Figure 8 shows a comparison of the Pb isotopic variations in the Reykjanes Peninsula lavas with those in the offshore Reykjanes Ridge mid-ocean ridge lavas (data from Thirlwall et al. 2004; Blichert-Toft et al. 2005; this paper). Both groups of samples define reasonably linear arrays on a plot of $^{206}\text{Pb}/^{204}\text{Pb}$ versus $^{208}\text{Pb}/^{204}\text{Pb}$ (Fig. 8b), but the Reykjanes Ridge samples have a steeper slope than the Reykjanes Peninsula lavas. This means that at low $^{206}\text{Pb}/^{204}\text{Pb}$ values, the Reykjanes Ridge samples have lower $^{208}\text{Pb}/^{204}\text{Pb}$ values than the Reykjanes Peninsula samples (consistent with the observations of Thirlwall et al. 2004). The radiogenic end of the Reykjanes Ridge array intersects the Reykjanes Peninsula array at an intermediate point that Thirlwall et al. (2004) defined as the Reykjanes Ridge Enriched (RRE) component. This is more clearly illustrated on the plot of $^{206}\text{Pb}/^{204}\text{Pb}$ versus $\Delta^{208}\text{Pb}$ (Fig. 8d). The fact that the RRE component lies at a point in the middle of the Reykjanes Peninsula data field led Thirlwall et al. (2004) to argue that the two local mixing end-members responsible for the Reykjanes Peninsula trend must have been well-mixed prior to their advection down the ridge and furthermore that this must have occurred at mantle depths.

Figure 8d shows that $\Delta^{208}\text{Pb}$ can only be used to clearly distinguish Reykjanes Peninsula and Reykjanes Ridge compositions that have $^{206}\text{Pb}/^{204}\text{Pb}$ values less than ~ 18.6 . Moving south down the Reykjanes Ridge, the first samples that have Pb isotope compositions that are resolvable from

the Reykjanes Peninsula lavas are found south of 62.4°N , with $^{206}\text{Pb}/^{204}\text{Pb} < 18.6$ and $\text{Nb}/\text{Zr} < 0.08$. The ridge section between 62.4°N and the Iceland coast at 63.8°N , a distance of ~ 200 km, contains samples with compositions transitional between the historic Reykjanes Peninsula lavas and true Reykjanes Ridge compositions ($^{206}\text{Pb}/^{204}\text{Pb}$ 18.6–18.7, Nb/Zr 0.08–0.10), although there is one sample (186D2: Thirlwall et al. 2004) that is similar in composition to the onshore historic lavas ($^{206}\text{Pb}/^{204}\text{Pb}$ 18.83, Nb/Zr 0.124). This poorly sampled region clearly represents an important transition zone.

On the Reykjanes Peninsula, samples with $^{206}\text{Pb}/^{204}\text{Pb} < 18.6$ and Pb isotope compositions distinct from the Reykjanes Ridge lavas all have ‘depleted’ compositions ($\text{Nb}/\text{Zr} < 0.08$; Fig. 9). Gee et al. (1998a) showed that the eruption of lavas with $\text{Nb}/\text{Zr} < 0.08$ and $^{206}\text{Pb}/^{204}\text{Pb} < 18.6$ was restricted to the interval between 9,000 and 13,000 years ago, a period in which the ice sheets that covered the Reykjanes Peninsula during the Weichselian glaciation disappeared. In most of the volcanic systems within Iceland, this deglaciation period has been recognised as a time of increased volcanic activity (e.g. Jakobsson et al. 1978; Gee et al. 1998a; Maclennan et al. 2002). Ice unloading affected both the state of stress within the crust and also the processes of melt generation within the mantle. Jull and McKenzie (1996) modelled how the unloading increased melt production through mantle decompression: the largest increase in melt production occurred at depths of about 60 km where the mantle had already been depleted by $\sim 15\%$ melting. Thus, the deglaciation interval should have been characterised by increased production and release of incompatible-element-depleted melts from the shallow, depleted mantle. Under normal conditions, such melts would have little compositional leverage and would be overwhelmed by incompatible-element-enriched melts derived either from melting of fertile enriched veins or streaks or from initial deep melting of the refractory peridotitic matrix. This is consistent with the modelling of platinum group element abundances in Icelandic lavas by Momme et al. (2003) who concluded that the ‘depleted’ picrites formed when unique tectonic conditions (i.e. glacial rebound) allowed the selective tapping of melts from the shallow, depleted central part of a triangular melting regime without contributions from low degree melts from the flanks and deeper levels of the melt generation zone.

It is worth noting that in the absence of the deglaciation event, ‘depleted’ melts with $^{206}\text{Pb}/^{204}\text{Pb} < 18.6$ would not be represented in the Reykjanes Peninsula lavas, except perhaps as melt inclusions trapped in early formed olivines (e.g. Gurenko and Chaussidon 1995; Maclennan 2008). Instead, the RRE component would be considered to be the end-member to both the Reykjanes Peninsula and Reykjanes Ridge compositional trends and thus an important

component within the Icelandic mantle, despite its clearly hybrid origin. The eruption of ‘depleted’ picrites during the deglaciation interval represents a good example of how surface processes can influence the sampling of compositional heterogeneities within the mantle.

Summary

Historic eruptions of tholeiitic basalts (MgO 6.5–9.2 wt%) on the Reykjanes Peninsula, Iceland, took place in a short time period between c. 940 and c. 1340 AD. They have a restricted composition variation in terms of incompatible trace element ratios and isotope ratios compared to earlier Reykjanes Peninsula lavas. High-precision double-spike Pb isotope data show coherent linear trends and good correlations with incompatible trace element ratios, indicating the importance of binary mixing processes. Poor correlations of Pb isotopes and incompatible trace element ratios with element concentrations show that mixing occurred prior to extensive fractional crystallisation. Pb isotope data on the older post-glacial Reykjanes Peninsula magmatism extend to much lower $^{206}\text{Pb}/^{204}\text{Pb}$ values than in the historic lavas. These earlier trace-element-depleted samples show significant heterogeneity in $^{207}\text{Pb}/^{204}\text{Pb}$ and $^{208}\text{Pb}/^{204}\text{Pb}$, which requires the involvement of at least three compositionally distinct components within the local mantle.

Acknowledgments We thank John Bailey, Jørn Kystol, Nick Rogers, and Terry Plank for providing the XRF and ICP-MS data, and Kresten Breddam and Ole Stecher, for kindly providing some of the samples and for numerous discussions on Icelandic geology. This work was funded primarily by the Danish National Research Foundation through a grant to the now defunct Danish Lithosphere Centre, and the oxygen isotope analyses were funded from start-up funds to DWP from the University of Iowa. DWP would also like to thank the University of Iowa for support during manuscript preparation, initially through an Old Gold Summer Fellowship and subsequently through a Scholar appointment at the Obermann Center for Advanced Studies. John MacLennan and an anonymous reviewer are thanked for their careful and thorough journal reviews which helped us to clarify several aspects of the presentation of our ideas.

References

- Abouchami W, Galer SJG, Hofmann AW (2000) High precision lead isotope systematics of lavas from the Hawaiian Scientific Drilling Project. *Chem Geol* 169:187–209. doi:10.1016/S0009-2541(00)00328-4
- Anders E, Grevesse N (1989) Abundances of the elements: meteoritic and solar. *Geochim Cosmochim Acta* 53:197–214. doi:10.1016/0016-7037(89)90286-X
- Baker JA, Waight TE, Ulfbeck DJ (2002) Rapid and highly reproducible analysis of rare earth elements by multiple collector ICP-MS. *Geochim Cosmochim Acta* 66:3635–3646. doi:10.1016/S0016-7037(02)00921-3
- Baker JA, Peate DW, Waight TE, Meyzen C (2004) Pb isotopic analysis of standards and samples using a ^{207}Pb – ^{204}Pb spike and thallium to correct for mass bias with a double-focusing MC–ICP-MS. *Chem Geol* 211:275–303. doi:10.1016/j.chemgeo.2004.06.030
- Baker JA, Peate DW, Thirlwall MF, Waight TE (2005) Reply to comment by Albarède et al. on “Pb isotopic analysis of standards and samples using a ^{207}Pb – ^{204}Pb spike and thallium to correct for mass bias with a double-focusing MC–ICP-MS”. *Chem Geol* 217:175–179. doi:10.1016/j.chemgeo.2004.12.002
- Bindeman IN, Sigmarsson O, Eiler J (2006) Time constraints on the origin of large volume basalts derived from O-isotope and trace element mineral zoning and U-series disequilibria in the Laki and Grímsvötn volcanic system. *Earth Planet Sci Lett* 245:245–259. doi:10.1016/j.epsl.2006.02.029
- Blichert-Toft J, Agranier A, Andres M, Kingsley R, Schilling J-G, Albarède F (2005) Geochemical segmentation of the Mid-Atlantic Ridge north of Iceland and ridge–hot spot interaction in the North Atlantic. *Geochem Geophys Geosyst* 6(1), Q01E19. doi:10.1029/2004GC000788
- Brandon AD, Graham DW, Waight TE, Gautason B (2007) ^{186}Os and ^{187}Os enrichments and high- $^3\text{He}/^4\text{He}$ sources in the Earth’s mantle: evidence from Icelandic picrites. *Geochim Cosmochim Acta* 71:4570–4591. doi:10.1016/j.gca.2007.07.015
- Burnard P, Harrison D (2005) Argon isotope constraints on modification of oxygen isotopes in Iceland basalts by surficial processes. *Chem Geol* 216:143–156. doi:10.1016/j.chemgeo.2004.11.001
- Chauvel C, Hémond C (2000) Melting of a complete section of recycled oceanic crust: trace element and Pb isotopic evidence from Iceland. *Geochem Geophys Geosyst* 1. doi:10.1029/1999GC000002
- Clifton AE, Kattenhorn SA (2006) Structural architecture of a highly oblique divergent plate boundary segment. *Tectonophysics* 419:27–40. doi:10.1016/j.tecto.2006.03.016
- Condomines M, Grönvold K, Hooker PJ, Muehlenbachs K, O’Nions RK, Oskarsson N et al (1983) Helium, oxygen, strontium and neodymium isotopic relationships in Icelandic volcanics. *Earth Planet Sci Lett* 66:25–136. doi:10.1016/0012-821X(83)90131-0
- Eiler JM (2001) Oxygen isotope variations of basaltic lavas and upper mantle rocks. *Rev Miner Geochem* 43:319–364. doi:10.2138/gsrmg.43.1.319
- Eiler JM, Grönvold K, Kitchen N (2000) Oxygen isotope evidence for the origin of chemical variations in lavas from Theistareykir volcano in Iceland’s northern volcanic zone. *Earth Planet Sci Lett* 184:269–286. doi:10.1016/S0012-821X(00)00318-6
- Einarsson S, Johannesson H, Sveinbjörnsdóttir AE (1991) *Krisuvikureldar II: Kapelluhraun og gatan um aldur Hellnahrauns*. Jökull 41:61–78 (in Icelandic)
- Eisele J, Sharma M, Galer SJG, Blichert-Toft J, Devey CW, Hofmann AW (2002) The role of sediment recycling in EM-1 inferred from Os, Pb, Hf, Nd, Sr isotope and trace element systematics of the Pitcairn hotspot. *Earth Planet Sci Lett* 196:197–212. doi:10.1016/S0012-821X(01)00601-X
- Eisele J, Abouchami W, Galer SJG, Hofmann AW (2003) The 320 kyr Pb isotope evolution of Mauna Kea lavas recorded in the HSDP-2 drill core. *Geochem Geophys Geosyst* 4(5):8710. doi:10.1029/2002GC0000339
- Elderfield H, Greaves MJ (1981) Strontium isotope geochemistry of Icelandic geothermal systems and implications for sea water chemistry. *Geochim Cosmochim Acta* 45:2201–2212. doi:10.1016/0016-7037(81)90072-7
- Elliott TR, Hawkesworth CJ, Grönvold K (1991) Dynamic melting of the Iceland plume. *Nature* 351:201–206. doi:10.1038/351201a0
- Fisk MR, Schilling JG, Sigurdsson H (1980) An experimental investigation of Iceland and Reykjanes Ridge tholeiites, I: phase

- relations. *Contrib Mineral Petrol* 74:361–374. doi:[10.1007/BF00518117](https://doi.org/10.1007/BF00518117)
- Fitton JG, Saunders AD, Norry MJ, Hardarson BS, Taylor RN (1997) Thermal and chemical structure of the Iceland plume. *Earth Planet Sci Lett* 153:197–208. doi:[10.1016/S0012-821X\(97\)00170-2](https://doi.org/10.1016/S0012-821X(97)00170-2)
- Fitton JG, Saunders AD, Kempton PD, Hardarson BS (2003) Does depleted mantle form an intrinsic part of the Iceland plume? *Geochim Geophys Geosyst* 4(3):1032. doi:[10.1029/2002GC0000424](https://doi.org/10.1029/2002GC0000424)
- Geer MAM, Taylor RN, Thirlwall MF, Murton BJ (1998a) Glacio-isostasy controls chemical and isotopic characteristics of tholeiites from the Reykjanes Peninsula, SW Iceland. *Earth Planet Sci Lett* 164:1–5. doi:[10.1016/S0012-821X\(98\)00246-5](https://doi.org/10.1016/S0012-821X(98)00246-5)
- Geer MAM, Thirlwall MF, Taylor RN, Lowry D, Murton BJ (1998b) Crustal processes: major controls on Reykjanes Peninsula lava chemistry, SW Iceland. *J Petrol* 39:819–839. doi:[10.1093/ptrology/39.5.819](https://doi.org/10.1093/ptrology/39.5.819)
- Geer MAM, Taylor RN, Thirlwall MF, Murton BJ (2000) Axial magma reservoirs located by variation in lava chemistry along Iceland's mid-ocean ridge. *Geology* 28:699–702. doi:[10.1130/0091-7613\(2000\)28and<699:AMRLBVand>2.0.CO;2](https://doi.org/10.1130/0091-7613(2000)28and<699:AMRLBVand>2.0.CO;2)
- Gudmundsson A (1986) Mechanical aspects of postglacial volcanism and tectonics of the Reykjanes Peninsula, southwest Iceland. *J Geophys Res* 91:12711–12721. doi:[10.1029/JB091iB12p12711](https://doi.org/10.1029/JB091iB12p12711)
- Gurenko AA, Chaussidon M (1995) Enriched and depleted primitive melts included in olivines from Icelandic tholeiites: origin by continuous melting of a single mantle column. *Geochim Cosmochim Acta* 59:2905–2917. doi:[10.1016/0016-7037\(95\)00184-0](https://doi.org/10.1016/0016-7037(95)00184-0)
- Gurenko AA, Sobolev AV (2006) Crust-primitive magma interaction beneath neovolcanic rift of Iceland recorded in gabbro xenoliths from Midfell, SW Iceland. *Contrib Mineral Petrol* 151:495–520. doi:[10.1007/s00410-006-0079-2](https://doi.org/10.1007/s00410-006-0079-2)
- Hanan BB, Schilling J-G (1997) The dynamic evolution of the Iceland mantle plume: the Pb isotope perspective. *Earth Planet Sci Lett* 151:43–60. doi:[10.1016/S0012-821X\(97\)00105-2](https://doi.org/10.1016/S0012-821X(97)00105-2)
- Hanan BB, Blichert-Toft J, Kingsley R, Schilling J-G (2000) Depleted Iceland mantle plume geochemical signature: artifact of multicomponent mixing? *Geochim Geophys Geosyst* 1. doi:[10.1029/1999GC000009](https://doi.org/10.1029/1999GC000009)
- Hardarson BS, Fitton JG, Ellam RM, Pringle MS (1997) Rift relocation—a geochemical and geochronological investigation of a palaeo-rift in northwest Iceland. *Earth Planet Sci Lett* 153:181–196. doi:[10.1016/S0012-821X\(97\)00145-3](https://doi.org/10.1016/S0012-821X(97)00145-3)
- Hart SR (1984) A large-scale isotope anomaly in the southern hemisphere mantle. *Nature* 309:753–757. doi:[10.1038/309753a0](https://doi.org/10.1038/309753a0)
- Hart SR, Schilling J-G, Powell JL (1973) Basalts from Iceland and along the Reykjanes Ridge: Sr isotope geochemistry. *Nat Phys Sci* 246:104–107
- Hémond C, Arndt NT, Lichtenstein U, Hofmann AW (1993) The heterogeneous Iceland mantle plume: Nd–Sr–O isotopes and trace element constraints. *J Geophys Res* 98:15833–15850. doi:[10.1029/93JB01093](https://doi.org/10.1029/93JB01093)
- Hilton DR, Grönvold K, Macpherson CG, Castillo PR (1999) Extreme $^3\text{He}/^4\text{He}$ ratios in northwest Iceland: constraining the common component in mantle plumes. *Earth Planet Sci Lett* 173:53–60. doi:[10.1016/S0012-821X\(99\)00215-0](https://doi.org/10.1016/S0012-821X(99)00215-0)
- Holm PM, Wilson JR, Christensen BP, Hansen L, Hansen SL, Hein KM et al (2006) Sampling the Cape Verde mantle plume: evolution of melt compositions on Santo Antão, Cape Verde islands. *J Petrol* 47:145–189. doi:[10.1093/ptrology/egi071](https://doi.org/10.1093/ptrology/egi071)
- Jakobsson SP (1974) Volcanic eruptions at Eldeyjárbodi, the Reykjanes Ridge. *Naturufraedingurinn* 44:22–44 (in Icelandic)
- Jakobsson SP, Jónsson J, Shido F (1978) Petrology of the western Reykjanes Peninsula, Iceland. *J Petrol* 19:669–705. doi:[10.1093/ptrology/19.4.669](https://doi.org/10.1093/ptrology/19.4.669)
- Jakobsson SP, Johnson GL, Moore JG (2000) A structural and geochemical study of the Western Volcanic Zone, Iceland: preliminary results. *InterRidge News* 9:27–33
- Johnson GL, Jakobsson SP (1985) Structure and petrology of the Reykjanes Ridge between 62°55'N and 63°48'N. *J Geophys Res* 90:10073–10083. doi:[10.1029/JB090iB12p10073](https://doi.org/10.1029/JB090iB12p10073)
- Jónsson J (1978) Geological map of Reykjaneskagi. Orkustofnun OSJHD 7831, 303 p + map (in Icelandic)
- Jónsson J (1983) Volcanic eruptions in historical times on the Reykjanes Peninsula, south-west Iceland. *Naturufraedingurinn* 52:127–139 (in Icelandic)
- Jull M, McKenzie DP (1996) The effect of deglaciation on mantle melting beneath Iceland. *J Geophys Res* 101:21815–21828. doi:[10.1029/96JB01308](https://doi.org/10.1029/96JB01308)
- Kadko D, Grönvold K, Butterfield D (2007) Application of radium isotopes to determine crustal residence times of hydrothermal fluids from two sites on the Reykjanes Peninsula, Iceland. *Geochim Cosmochim Acta* 71:6019–6029. doi:[10.1016/j.gca.2007.09.018](https://doi.org/10.1016/j.gca.2007.09.018)
- Kamber BS, Collerson KD (2000) Zr/Nb systematics of ocean island basalts reassessed—the case for binary mixing. *J Petrol* 41:1007–1021. doi:[10.1093/ptrology/41.7.1007](https://doi.org/10.1093/ptrology/41.7.1007)
- Kelley DF, Barton M (2008) Pressures of crystallization of Icelandic magmas. *J Petrol* 49:465–492. doi:[10.1093/ptrology/egm089](https://doi.org/10.1093/ptrology/egm089)
- Kelley KA, Plank T, Ludden J, Staudigel H (2003) Composition of altered oceanic crust at ODP Sites 801 and 1149. *Geochim Geophys Geosyst* 4(6):8910. doi:[10.1029/2002GC000435](https://doi.org/10.1029/2002GC000435)
- Kempton PD, Fitton JG, Saunders AD, Nowell GM, Taylor RN, Hardarson BS et al (2000) The Iceland plume in space and time: a Sr–Nd–Pb–Hf study of the North Atlantic rifted margin. *Earth Planet Sci Lett* 177:255–271. doi:[10.1016/S0012-821X\(00\)00047-9](https://doi.org/10.1016/S0012-821X(00)00047-9)
- Kent AJR, Clague DA, Honda M, Stolper EM, Hutcheon ID, Norman MD (1999) Widespread assimilation of a seawater-derived component at Loihi seamount, Hawaii. *Geochim Cosmochim Acta* 63:2749–2761. doi:[10.1016/S0016-7037\(99\)00215-X](https://doi.org/10.1016/S0016-7037(99)00215-X)
- Kerr AC, Saunders AD, Tarney J, Berry NH, Hards VL (1995) Depleted mantle plume geochemical signature: no paradox for plume theories. *Geology* 23:843–846. doi:[10.1130/0091-7613\(1995\)023and<0843:DMPGSNand>2.3.CO;2](https://doi.org/10.1130/0091-7613(1995)023and<0843:DMPGSNand>2.3.CO;2)
- Kokfelt TF, Hoernle K, Hauff F (2003) Upwelling and melting of the Iceland plume from radial variation of U-238–Th-230 disequilibria in postglacial volcanic rocks. *Earth Planet Sci Lett* 214, 167–186. doi:[10.1016/S0012-821X\(03\)00306-6](https://doi.org/10.1016/S0012-821X(03)00306-6)
- Kokfelt TF, Hoernle K, Hauff F, Fiebig J, Werner R, Garbeschönberg D (2006) Combined trace element and Pb–Nd–Sr–O isotope evidence for recycled oceanic crust (upper and lower) in the Iceland mantle plume. *J Petrol* 47:1705–1749. doi:[10.1093/ptrology/egi025](https://doi.org/10.1093/ptrology/egi025)
- Kurz MD, Meyer H, Sigurdsson H (1985) Helium isotopic systematics within the neovolcanic zones of Iceland. *Earth Planet Sci Lett* 74:291–305. doi:[10.1016/S0012-821X\(85\)80001-7](https://doi.org/10.1016/S0012-821X(85)80001-7)
- Kystol J, Larsen LM (1999) Analytical procedures in the rock geochemical laboratory of the Geological Survey of Denmark and Greenland. *Geol Greenl Surv Bull* 184:59–62
- Larsen LM, Pedersen AK (2000) Processes in high-Mg, high-T magmas: evidence from olivine, chromite and glass in Palaeogene picrites from West Greenland. *J Petrol* 41:1071–1098. doi:[10.1093/ptrology/41.7.1071](https://doi.org/10.1093/ptrology/41.7.1071)
- Langmuir CH, Vocke RD, Hanson GN, Hart SR (1978) A general mixing equation with applications to Icelandic basalts. *Earth Planet Sci Lett* 37:380–392. doi:[10.1016/0012-821X\(78\)90053-5](https://doi.org/10.1016/0012-821X(78)90053-5)

- Lundstrom CC, Williams Q, Gill JB (1998) Investigating solid mantle upwelling rates beneath mid-ocean ridges using U-series disequilibria, 1: a global approach. *Earth Planet Sci Lett* 157:151–165. doi:10.1016/S0012-821X(98)00038-7
- MacLennan J (2008) Lead isotope variability in olivine-hosted melt inclusions from Iceland. *Geochim Cosmochim Acta* 72:4159–4176. doi:10.1016/j.gca.2008.05.034
- MacLennan J, Jull M, McKenzie DP, Slater L, Grönvold K (2002) The link between volcanism and deglaciation in Iceland. *Geochem Geophys Geosyst* 3(11):1062. doi:10.1029/2000GC000282
- MacLennan J, McKenzie DP, Hilton F, Grönvold K, Shimizu N (2003a) Geochemical variability in a single flow from northern Iceland. *J Geophys Res* 108(B1), 2007. doi:10.1029/2000JB000142
- MacLennan J, McKenzie DP, Grönvold K, Shimizu N, Eiler JM, Kitchen N (2003b) Melt mixing and crystallisation under Theistareykir, northeast Iceland. *Geochem Geophys Geosyst* 4(11):8624. doi:10.1029/2003GC000558
- Martin E, Sigmarsson O (2005) Trondhjemitic and granitic melts formed by fractional crystallization of an olivine tholeiite from Reykjanes Peninsula, Iceland. *Geol Mag* 142:651–658. doi:10.1017/S0016756805001160
- Mattey DP, Macpherson C (1993) High-precision oxygen isotope microanalysis of ferromagnesian minerals by laser fluorination. *Chem Geol* 105:305–318. doi:10.1016/0009-2541(93)90133-4
- Mattey DP, Lowry D, Macpherson C (1994) Oxygen isotope composition of mantle peridotite. *Earth Planet Sci Lett* 128:231–241. doi:10.1016/0012-821X(94)90147-3
- Momme P, Oskarsson N, Keys RR (2003) Platinum-group elements in the Icelandic rift system: melting processes and mantle sources beneath Iceland. *Chem Geol* 196:209–234. doi:10.1016/S0009-2541(02)00414-X
- Muehlenbachs K, Anderson AT, Sigvaldason GE (1974) Low-¹⁸O basalts from Iceland. *Geochim Cosmochim Acta* 38:577–588. doi:10.1016/0016-7037(74)90042-8
- Murray RW, Miller DJ, Kryc KA (2000). Analysis of major and trace elements in rocks, sediments, and interstitial waters by inductively coupled plasma atomic emission spectrometry (ICP-AES). ODP Technology Note, 29 (online). Available from World Wide Web: <<http://www.odp.tamu.edu/publications/tnotes/th29/index.htm>>
- Murton BJ, Taylor RN, Thirlwall MF (2002) Plume-ridge interaction: a geochemical perspective from the Reykjanes Ridge. *J Petrol* 43:1987–2012. doi:10.1093/petrology/43.11.1987
- Nielsen SG, Rehkämper M, Brandon AD, Norman MD, Turner SP, O'Reilly SY (2007) Thallium isotopes in Iceland and Azores lavas—implications for the role of altered crust and mantle geochemistry. *Earth Planet Sci Lett* 264:332–345. doi:10.1016/j.epsl.2007.10.008
- Nimis P, Ulmer P (1998) Clinopyroxene geobarometry of magmatic rocks, part 1: an expanded structural geobarometer for anhydrous and hydrous, basic and ultrabasic systems. *Contrib Mineral Petrol* 133:122–135. doi:10.1007/s004100050442
- Norrish K, Chappell BW (1967) X-ray fluorescence spectrometry. In: Zussman J (ed) *Physical methods in determinative mineralogy*. Academic Press, New York, pp 161–214
- Oskarsson N, Helgason Ö, Steinthorsson S (1994) Oxidation state of iron in mantle-derived magmas of the Icelandic rift zone. *Hyperfine Interact* 91:733–737. doi:10.1007/BF02064599
- Peate DW, Hawkesworth CJ, van Calsteren PW, Taylor RN, Murton BJ (2001) ²³⁸U–²³⁰Th constraints on mantle upwelling and plume–ridge interaction along the Reykjanes Ridge. *Earth Planet Sci Lett* 187:259–272. doi:10.1016/S0012-821X(01)00266-7
- Peate DW, Baker JA, Blichert-Toft J, Hilton DR, Storey M, Kent AJR et al (2003) The Prinsen af Wales Bjerge Formation lavas, East Greenland: the transition from tholeiitic to alkalic magmatism during Palaeogene continental break-up. *J Petrol* 44:279–304. doi:10.1093/petrology/44.2.279
- Putirka KD (1997) Magma transport at Hawaii: inferences based on igneous thermobarometry. *Geology* 25:69–72. doi:10.1130/0091-7613(1997)025and>0069:MTAHIBand<2.3.CO;2
- Putirka KD (2005) Mantle potential temperature at Hawaii, Iceland and the mid-ocean ridge system as inferred from olivine phenocrysts: evidence for thermally diverse mantle plumes. *Geochem Geophys Geosyst* 6(5):Q05L08. doi:10.1029/2005GC000915
- Putirka K, Johnson M, Kinzler R, Longhi J, Walker D (1996) Thermobarometry of mafic igneous rocks based in clinopyroxene–liquid equilibria, 0–30 kbar. *Contrib Mineral Petrol* 123:92–108. doi:10.1007/s004100050145
- Reiners PW (2002) Temporal-compositional trends in intraplate basalt eruptions: implications for mantle heterogeneity and melting processes. *Geochem Geophys Geosyst* 3(2). doi:10.1029/2001GC000250
- Révilion S, Arndt NT, Hallot E, Kerr AC, Tarney J (1999) Petrogenesis of picrites from the Caribbean Plateau and the North Atlantic magmatic province. *Lithos* 49:1–21. doi:10.1016/S0024-4937(99)00038-9
- Rogers NW, Thomas LE, Macdonald R, Hawkesworth CJ, Mokadem F (2006) ²³⁸U–²³⁰Th disequilibrium in recent basalts and dynamic melting beneath the Kenya rift. *Chem Geol* 234:148–168. doi:10.1016/j.chemgeo.2006.05.002
- Saal AE, Hart SR, Shimizu N, Hauri EH, Layne GD (1998) Pb isotopic variability in melt inclusions from oceanic island basalts, Polynesia. *Science* 282:278–281. doi:10.1126/science.282.5393.1481
- Schilling J-G, Kingsley R, Fontignie D, Poreda R, Xue S (1999) Dispersion of the Jan Mayen and Iceland mantle plumes in the Arctic: a He–Pb–Nd–Sr isotope tracer study of basalts from the Kolbeinsey, Mohns and Knipovich Ridges. *J Geophys Res* 104:10543–10569. doi:10.1029/1999JB900057
- Sigmarsson O, Condomines M, Grönvold K, Thordarson T (1991) Extreme magma homogeneity in the 1784–84 Lakagigar eruption—origin of a large volume of evolved basalt in Iceland. *Geophys Res Lett* 18:2229–2232. doi:10.1029/91GL02328
- Sigmarsson O, Condomines M, Fourcade F (1992) Mantle and crustal contribution in the genesis of Recent basalts from off-ridge zones in Iceland: constraints from Th, Sr and O isotopes. *Earth Planet Sci Lett* 110:149–162. doi:10.1016/0012-821X(92)90045-W
- Sims KWW, Goldstein SJ, Blichert-Toft J, Perfitt MR, Kelemen P, Fornari DJ et al (2002) Chemical and isotopic constraints on the generation and transport of magma beneath the East Pacific Rise. *Geochim Cosmochim Acta* 66:3481–3504. doi:10.1016/S0016-7037(02)00909-2
- Sinton J, Grönvold K, Saemundsson K (2005) Postglacial eruptive history of the Western Volcanic Zone, Iceland. *Geochem Geophys Geosyst* 6(12):Q12009. doi:10.1029/2005GC001021
- Skovgaard AC, Storey M, Baker JA, Blusztajn J, Hart SR (2001) Osmium–oxygen isotopic evidence for a recycled and strongly depleted component in the Iceland mantle plume. *Earth Planet Sci Lett* 194:259–275. doi:10.1016/S0012-821X(01)00549-0
- Spiegelman M, Kelemen PB (2003) Extreme chemical variability as a consequence of channelized melt transport. *Geochem Geophys Geosyst* 4(7):1055–1522. doi:10.1029/2002GC000336
- Stecher O, Carlson RW, Shirey SB (1986) Sr and Nd isotopes and the petrological evolution of post-glacial lavas from the Reykjanes Peninsula, Iceland. *Eos Trans AGU* 67:413
- Stecher O, Carlson RW, Gunnarsson B (1999) Torfajökull: a radiogenic end-member of the Iceland Pb–isotopic array. *Earth Planet Sci Lett* 165:117–127. doi:10.1016/S0012-821X(98)00256-8

- Stracke A, Zindler A, Salters VJM, McKenzie D, Blichert-Toft J, Albarède F et al (2003) Theistareykir revisited. *Geochem Geophys Geosyst* 4(2):8507. doi:[10.1029/2001GC000201](https://doi.org/10.1029/2001GC000201)
- Sun S-S, Jahn B (1975) Lead and strontium isotopes in post-glacial basalts from Iceland. *Nature* 255:527–530. doi:[10.1038/255527a0](https://doi.org/10.1038/255527a0)
- Thirlwall MF, Gee MAM, Taylor RN, Murton BJ (2004) Mantle components in Iceland and adjacent ridges investigated using double-spike Pb isotope ratios. *Geochim Cosmochim Acta* 68:361–386. doi:[10.1016/S0016-7037\(03\)00424-1](https://doi.org/10.1016/S0016-7037(03)00424-1)
- Thirlwall MF, Gee MAM, Lowry D, Matthey DP, Murton BJ, Taylor RN (2006) Low $\delta^{18}\text{O}$ in the Icelandic mantle and its origins: evidence from Reykjanes Ridge and Icelandic lavas. *Geochim Cosmochim Acta* 70:993–1019. doi:[10.1016/j.gca.2005.09.008](https://doi.org/10.1016/j.gca.2005.09.008)
- Waight TE, Baker JA, Peate DW (2002) Sr isotope measurement by double focusing MC-ICP-MS: techniques, observations and pitfalls. *Int J Mass Spectrom* 221:229–244. doi:[10.1016/S1387-3806\(02\)01016-3](https://doi.org/10.1016/S1387-3806(02)01016-3)
- Weir NRW, White RS, Brandsdóttir B, Einarsson P, Shimamura H, Shiobara H, RISE fieldwork team (2001) Crustal structure of the northern Reykjanes Ridge and Reykjanes Peninsula, southwest Iceland. *J Geophys Res* 106:6347–6368. doi:[10.1029/2000JB900358](https://doi.org/10.1029/2000JB900358)
- Wood DA (1978) Major and trace element variations in the Tertiary lavas of eastern Iceland and their significance with respect to the Iceland geochemical anomaly. *J Petrol* 19:393–436. doi:[10.1093/petrology/19.3.393](https://doi.org/10.1093/petrology/19.3.393)
- Wood DA (1981) Partial melting models for the petrogenesis of Reykjanes Peninsula basalts, Iceland: implications for the use of trace elements and strontium and neodymium isotope ratios to record inhomogeneities in the upper mantle. *Earth Planet Sci Lett* 52:183–190. doi:[10.1016/0012-821X\(81\)90219-3](https://doi.org/10.1016/0012-821X(81)90219-3)
- Workman RK, Hart SR, Jackson M, Regelous M, Farley KA, Blusztajn J et al (2004) Recycled metasomatized lithosphere as the origin of the Enriched Mantle II (EM-2) end-member: evidence from the Samoan volcanic chain. *Geochem Geophys Geosyst* 5(4):Q04008. doi:[10.1029/2003GC0000623](https://doi.org/10.1029/2003GC0000623)
- Zindler A, Hart SR, Frey FA, Jakobsson SP (1979) Nd and Sr isotope ratios and rare earth element abundances in Reykjanes Peninsula basalts: evidence for mantle heterogeneity beneath Iceland. *Earth Planet Sci Lett* 45:249–262. doi:[10.1016/0012-821X\(79\)90127-4](https://doi.org/10.1016/0012-821X(79)90127-4)